UCRL-ID-141346

Femtosecond Laser Processing of Fuel Injectors-A Materials Processing Evaluation

B. C. Stuart, A. Wynne

December 16, 2000

U.S. Department of Energy

Lawrence
Livermore
National
Laboratory

Approved for public release; further dissemination unlimited

DISCLAIMER

This document was prepared as an account of work sponsored by an agency of the United States Government. Neither the United States Government nor the University of California nor any of their employees, makes any warranty, express or implied, or assumes any legal liability or responsibility for the accuracy, completeness, or usefulness of any information, apparatus, product, or process disclosed, or represents that its use would not infringe privately owned rights. Reference herein to any specific commercial product, process, or service by trade name, trademark, manufacturer, or otherwise, does not necessarily constitute or imply its endorsement, recommendation, or favoring by the United States Government or the University of California. The views and opinions of authors expressed herein do not necessarily state or reflect those of the United States Government or the University of California, and shall not be used for advertising or product endorsement purposes.

This work was performed under the auspices of the U. S. Department of Energy by the University of California, Lawrence Livermore National Laboratory under Contract No. W-7405-Eng-48.

This report has been reproduced directly from the best available copy.

Available electronically at http://www.doc.gov/bridge

Available for a processing fee to U.S. Department of Energy
And its contractors in paper from
U.S. Department of Energy
Office of Scientific and Technical Information
P.O. Box 62
Oak Ridge, TN 37831-0062
Telephone: (865) 576-8401
Facsimile: (865) 576-5728
E-mail: reports@adonis.osti.gov

Available for the sale to the public from
U.S. Department of Commerce
National Technical Information Service
5285 Port Royal Road
Springfield, VA 22161
Telephone: (800) 553-6847
Facsimile: (703) 605-6900
E-mail: orders@ntis.fedworld.gov
Online ordering: http://www.ntis.gov/ordering.htm

OR

Lawrence Livermore National Laboratory
Technical Information Department's Digital Library
http://www.llnl.gov/tid/Library.html

Femtosecond Laser Materials Processing Evaluation

Brent C. Stuart, Alexis Wynne
Lawrence Livermore National Laboratory

Work supported by DOE Project: FWP #EEW0066
Program Manager: Sidney Diamond

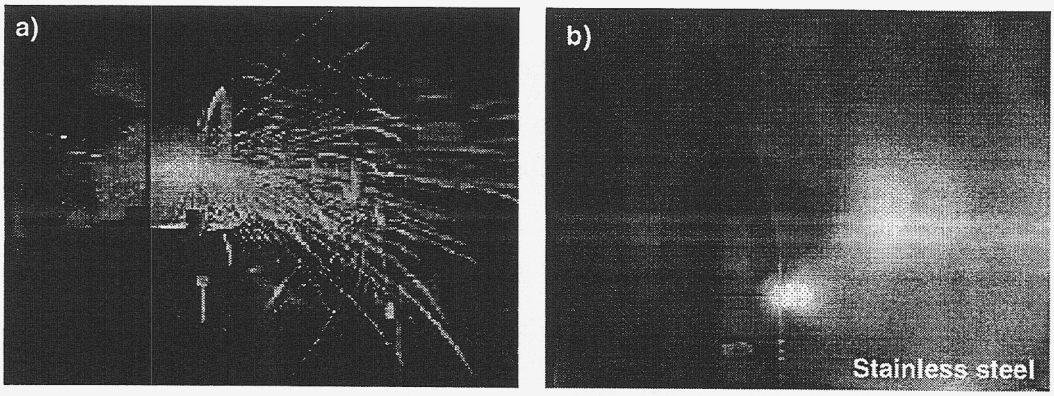

Figure 1.1. Machining of stainless steel with:
a) conventional lasers, and b) with ultrashort (10^{-13} sec) pulse lasers

TABLE OF CONTENTS

1. Introduction 3
   1.1 Femtosecond laser materials processing 3
   1.2 Application to fuel injectors 4
   1.3 Scope of Work 6

2. Air vs. Vacuum 7
   2.1 Introduction 7
   2.2 Experimental setup 7
   2.3 Initial ablation rates 8
   2.4 Through-hole drilling 12
   2.5 Discussion 30

3. Martensitic steel 31
   3.1 Introduction 31
   3.2 Samples 31
   3.3 Laser Drilling 31
   3.4 ORNL analysis 40
   3.5 LLNL Conclusions 44

4. Ceramics and Metal-matrix composite 45
   4.1 Alumina 45
   4.2 Zirconia 48
   4.3 Metal-matrix composite 49
   4.4 Conclusions 50

5. Summary and future directions 51
   5.1 Summary 51
   5.2 Materials processed by LLNL's femtosecond system 53
   5.3 Future directions 54

1. Introduction

1.1 Femtosecond laser materials processing

Lawrence Livermore National Laboratory (LLNL) has developed a new laser-based machining technology that utilizes ultrashort-pulse (0.1–1.0 picosecond) lasers to cut materials with negligible generation of heat or shock. The ultrashort pulse laser, developed for the Department of Energy (Defense Programs) has numerous applications in operations requiring high precision machining. Due to the extremely short duration of the laser pulse, material removal occurs by a different physical mechanism than in conventional machining. As a result, *any* material (e.g., hardened steel, ceramics, diamond, silicon, etc.) can be machined with minimal heat-affected zone or damage to the remaining material. As a result of the threshold nature of the process, shaped holes, cuts, and textures can be achieved with simple beam shaping.

Conventional laser tools used for cutting or high-precision machining (e.g., sculpting, drilling) use long laser pulses (10^{-8} to over 1 sec) to remove material by heating it to the melting or boiling point (Figure 1.1a). This often results in significant damage to the remaining material and produces considerable slag (Figure 1.2a). With ultrashort laser pulses, material is removed by ionizing the material (Figure 1.1b). The ionized plasma expands away from the surface too quickly for significant energy transfer to the remaining material. This distinct mechanism produces extremely precise and clean-edged holes without melting or degrading the remaining material (Figures 1.2 and 1.3). Since only a very small amount of material (≈<0.5 microns) is removed per laser pulse, extremely precise machining can be achieved. High machining speed is achieved by operating the lasers at repetition rates up to 10,000 pulses per second.

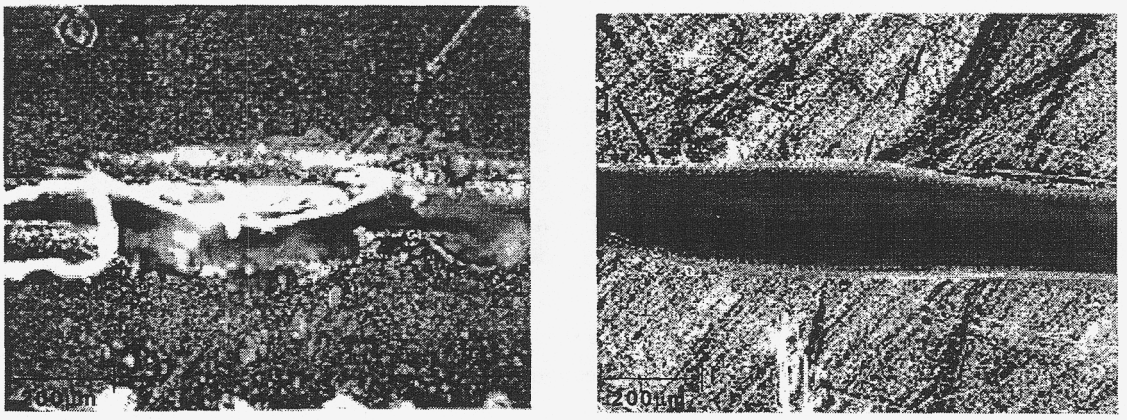

Figure 1.2: Top of cut in stainless steel performed with the same laser (wavelength =1 μm) operating with a) conventional pulses and b) ultrashort (10^{-13} sec) pulses.

As a diagnostic, the character of the short-pulse laser produced plasma enables determination of the material being machined between pulses. This feature allows the machining of multilayer materials, metal on metal or metal on ceramic where one

material can be machined without damaging the next. Developed originally for the Stockpile Stewardship program of the Department of Energy, numerous industrial, medical and national security applications of the technology have emerged.

The difference in machining ability of the ultrashort-pulse laser is dramatically illustrated in Figures 1.2 and 1.3. The clear presence of slag (resolidified molten material) is observable in Figure 1.2a where 1 mm thick stainless steel was cut with a 1 μm solid-state laser. By changing the pulse duration of the laser to the ultrashort regime ($\approx 10^{-13}$ to 10^{-12} sec), material is removed without melting and the formation of slag. A cross section of holes drilled in 304 stainless steel (Figure 1.3) illustrates the lack of any heat affected zone or collateral damage in the remaining material. Note that the individual grain boundaries are intact up to the edge of the laser-machined surface.

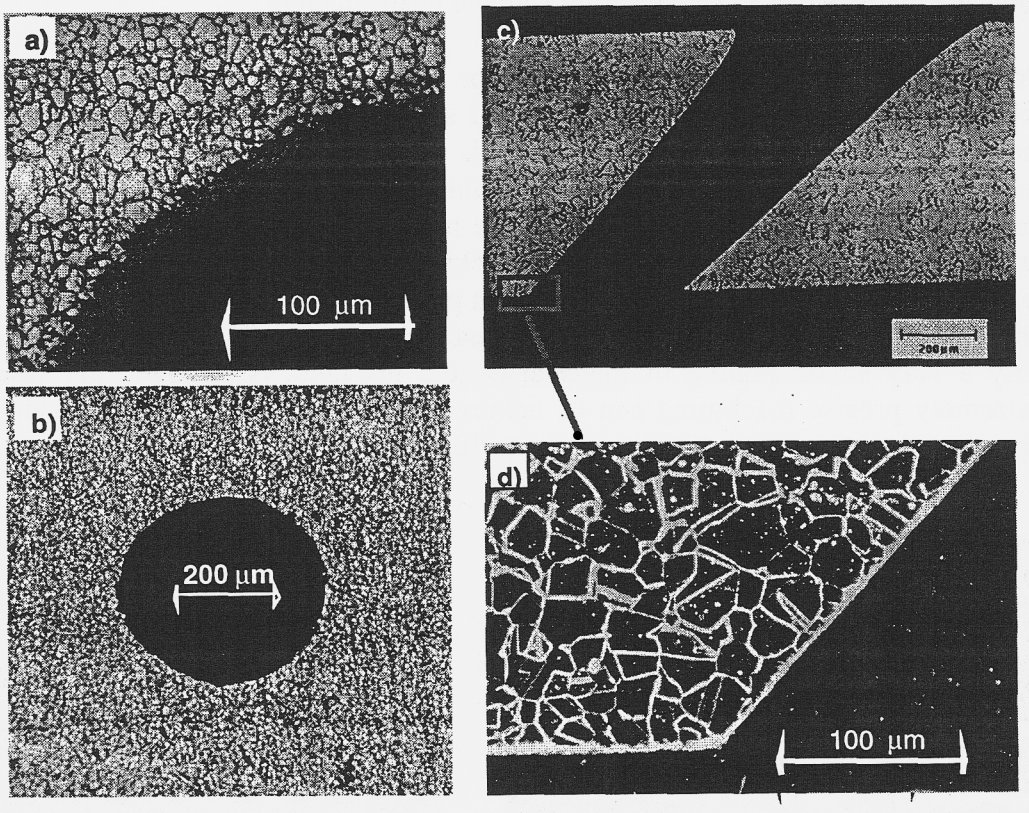

Figure 1.3. Holes drilled through 1 mm stainless steel with 120 fs laser pulses at 45°: a) Magnified section of top of hole, b) exit hole on bottom, c) cross section, d) magnified (bottom left) cross section.

1.2 Application to Fuel Injectors

Fuel injectors are commonly produced by electron discharge machining (EDM). It is difficult to produce high quality holes below a diameter of ≈0.2 mm through 1-mm thick steel with EDM. For these reasons, laser drilling has often been investigated. Clean, straight-walled holes with minimal heat affected zone have been produced by trepanning

with copper vapor lasers and frequency doubled Nd:YAG lasers. Trepanning is the process by which the laser beam is rotated around the hole. Laser drilling has been plagued by the problem of backwall damage associated with trepanning (Figure 1.4). Even if the backwall damage problem can be solved, it will be difficult to achieve the next generation of holes (diameter ≈100 microns) with conventional laser processing due to diffraction associated with the laser beam. Achieving this next generation of holes is critical for meeting the goals for improved fuel efficiency and reduced emissions. Increased fuel efficiency can be achieved by decreasing the hole size in the injector thereby increasing the atomization level of the fuel. An increase in fuel efficiency of only 1% would have a dramatic effect on the reduction of carbon dioxide emission from military vehicles and diesel generators.

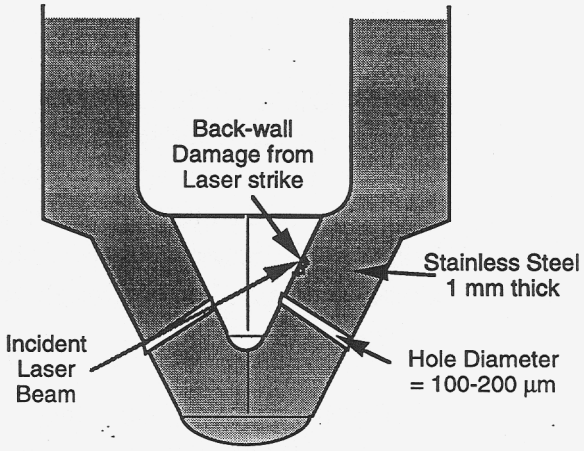

Figure 1.4
Typical fuel injector illustrating the problem of backwall damage in conventional laser processing

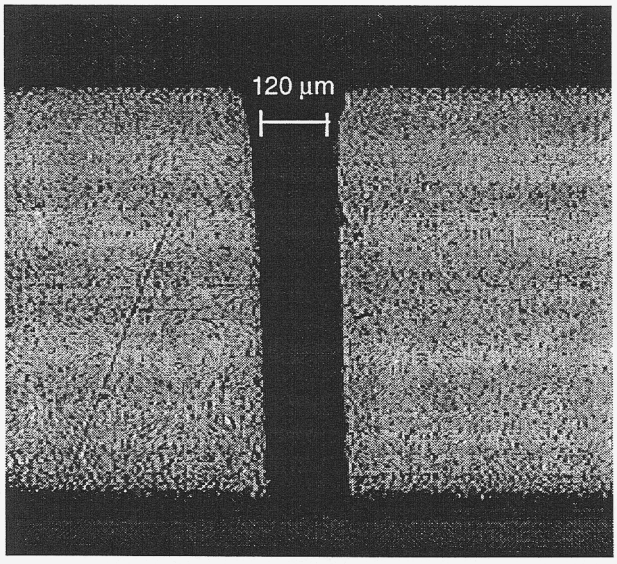

Figure 1.5
Injector hole produced by ultrashort-pulse laser Drilling (no trepanning)

By utilizing the rapid ionization machining mechanism associated with ultrashort-pulse laser machining, very clean holes of the size necessary for increased efficiency (≈0.1 mm) can be produced in fuel injector nozzles (Figure 1.5). These holes can be produced without trepanning and potentially no backwall damage (preliminary investigations are encouraging, but much work remains). Since ultrashort-pulse machining performs similarly in all materials, equivalent results can be produced in ceramics.

1.3 Scope of Work

Three areas were identified for initial investigation into the benefits of and practical implementation of femtosecond laser drilling for transportation-related applications:

1) Drilling in air vs. vacuum

Due to the short pulse duration, the peak intensity of each pulse is very high ($>10^{12}$ W/cm^2). This can lead to breakdown of air and usually requires drilling in a vacuum environment. Drilling in vacuum adds complexity to a high-throughput industrial process. What is the consequence of drilling in air instead of vacuum? We measured the initial ablation rates and drill-through times in 1-mm stainless steel as a function of fluence and pulse duration.

2) Drilling of martensitic steel

A simple experiment was designed to determine whether or not a heat effected zone surrounded holes drilled in steel foil by the femtosecond laser. LLNL drilled holes in specimens of a heat-resistant martensitic 9Cr-1MoVNb steel foils (supplied in two metallurgical conditions by ORNL) using a range of parameters with the femtosecond laser. ORNL then performed post-laser-drilling analysis with additional metallographic examination of the material surrounding the holes.

3) Drilling of ceramics

An initial investigation into drilling of ceramics was made.

The results are presented in the following three chapters.

2. Air vs. Vacuum

2.1 Introduction

Many micro-machining applications benefit from minimally invasive procedures that can precisely drill materials with little collateral damage to the surrounding material. Developments in ultrashort-pulse (sub-ps) laser technology have opened up a new regime of materials processing. Precise and reproducible drilling of nearly any material with minimal collateral damage has been demonstrated.

Much of the previous work in micro-drilling of metals with ultrashort-pulses has been done in a vacuum to prevent laser-air interactions. However, for many industrial applications, the ability to drill in air is desirable to cut down complexity and cost.

In this section we present ablation rates of stainless steel and aluminum at different pulse-widths in both air and vacuum. Although rates have previously been measured for various energies and fluences, to our knowledge no complete analysis of the differences between air and vacuum has been completed. It will be shown experimentally that the ablation rate of aluminum is much higher in vacuum at shorter pulse-widths. We discuss the effects the air environment has on the drilling rates and how the rates differ with pulse-width and fluence. We present data on how the ablation rates change as the hole deepens in the initial ablation regime (aspect ratio <2:1). We then measure the breakthrough times for drilling through 1-mm thick aluminum and stainless steel and show the resulting entrance and exit holes at breakthrough and after a "cleanup" time of five times the breakthrough time. This choice of "cleanup" time allows the process to reach a steady-state, after which not much happens to the hole shape.

2.2 Experimental setup

For the experiments described in this section, we used a chirped-pulse amplification (CPA) Ti:sapphire laser and amplifier system. The system delivered pulses at a repetition rate of 1 kHz with energies up to 5 mJ at a wavelength of 810 nm. Because of the CPA configuration, the pulse width could be varied from 150 fs to 20 ps without changing any other parameters. When a 500 ps pulse was needed, the uncompressed pulse was picked off and sent to the drilling chamber.

A lens of focal length 64 cm was used to focus the Gaussian beam to a round spot with a diameter of 400 microns. The polarization was made circular by adding a 1/4-wave plate, and the beam hit the part to be drilled at normal incidence. The fluence was changed by adjusting the power, while the spot size remained constant.

The parts drilled were 1" X 1" coupons of two materials, 304 stainless steel (900 microns thick), and 7075 aluminum (1 mm thick). When drilling in vacuum, the pressure in the chamber was approximately 10 mTorr. When drilled in air, the chamber was vented and the lid left off.

A fast mechanical shutter (UniBlitz) was used to select a defined number of pulses. For each fluence and pulse-width chosen, 6 holes were drilled, 2 holes for each of three different times (number of pulses). The times and corresponding number of pulses chosen were 0.5 s (500 pulses), 1 s (1000 pulses), and 2 s (2000 pulses). The depths of the two holes were averaged in each case and used to determine the drilling rate for that number of pulses. Then the three rates were averaged to get the final rate for each fluence. The estimated error in depth was ±10%, and in fluence ±15%.

The depths were measured with a light microscope with a calibrated z stage. The microscope was focused at the surface of the part and then zeroed. Then the focus was moved to the deepest surface of the hole and the depth recorded. The estimated uncertainty in depth was ±10%, and the uncertainty in fluence ±15%.

2.3 Initial ablation rates

At the shorter pulse-widths (150 fs, 1 ps) the drilling rate in vacuum exceeded the drilling rate in air for both materials, although the difference was greater for aluminum. (Figures 2.1 and 2.2) The rates were similar in both the 150 fs case and the 1 ps case. At 20 ps, the rates for all conditions were lower than the shorter pulse-widths. The rates for stainless steel were similar in air and vacuum while the rates for aluminum were higher in vacuum than in air. (Figure 2.3) At 500 ps, the rates are again lower than those at shorter pulse-widths. For lower fluences at 500 ps, the drilling rate of stainless steel was higher in air than in vacuum, but above 1 J/cm^2, the rate was higher in vacuum. For aluminum, the rate in air was higher than in vacuum for all fluences tested (Figure 2.4). This is the only pulse-width for which the ablation rate of aluminum was higher in air than in vacuum.

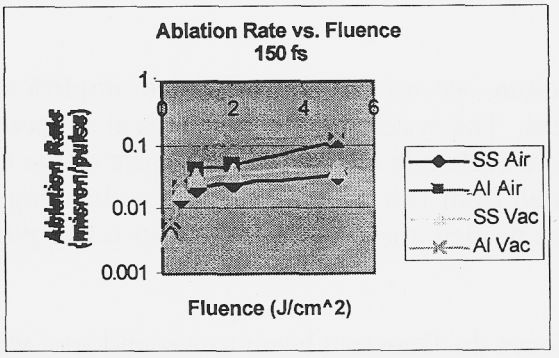

Fig. 2.1. Ablation Rate vs. Fluence at 150 fs for aluminum and stainless steel in air and vacuum.

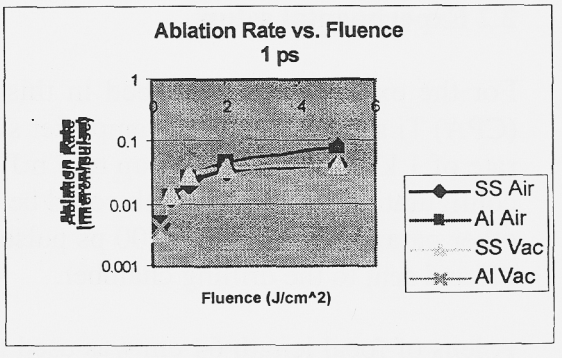

Fig. 2. 2. Ablation Rate vs. Fluence at 1 ps for aluminum and stainless steel in air and vacuum.

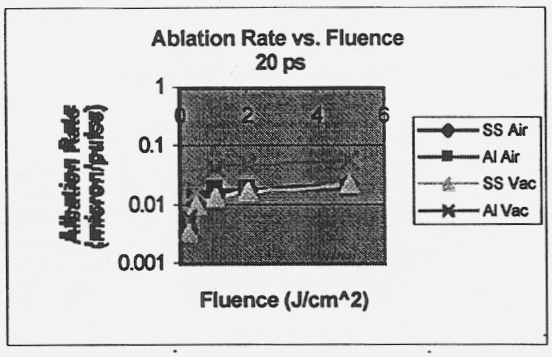

Fig. 2.3. Ablation Rate vs. Fluence at 20 ps for aluminum and stainless steel in air and vacuum.

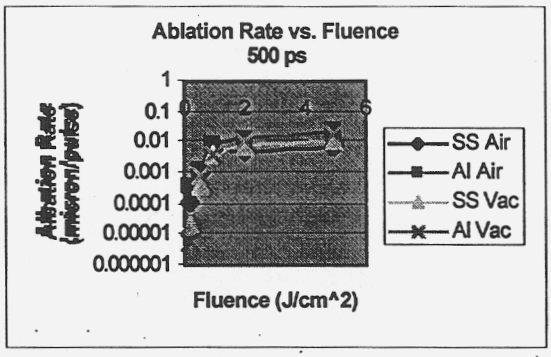

Fig.2.4. Ablation Rate vs. Fluence at 500 ps for aluminum and stainless steel in air and vacuum.

As part of the results above, we measured ablation rate as a function of hole depth. The general trend of this data is that rate decreases with depth. At higher pulse-widths, this decrease is sharper, especially for higher fluences. There is no appreciable difference of slope between holes drilled in air and holes drilled in vacuum. There is also no appreciable difference between stainless steel and aluminum. The decrease in rate with increased depth seems dependent only on pulse-width and fluence (see Figs. 2.5-2.8).

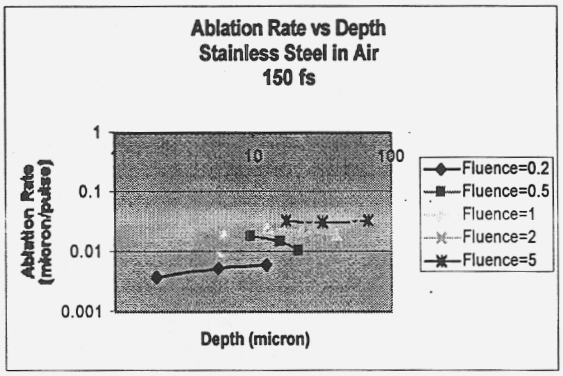

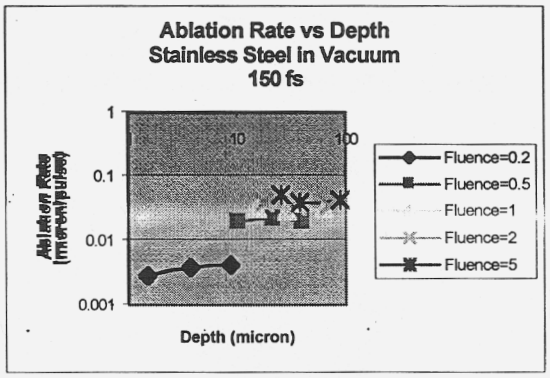

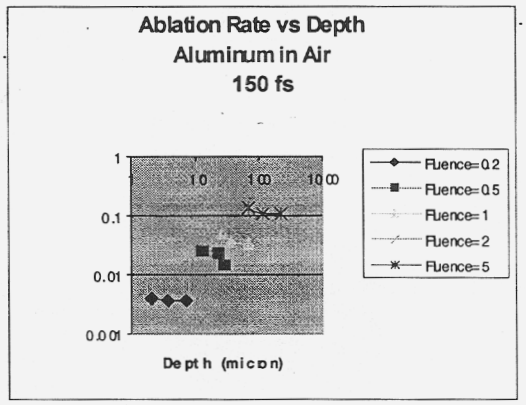

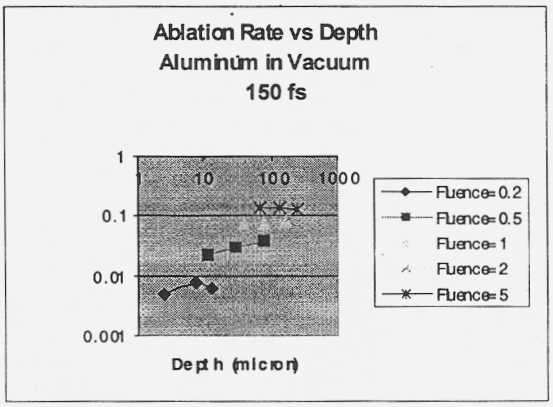

Figure 2.5 Ablation rate vs. hole depth at 0.15 ps for aluminum and stainless steel in air and vacuum.

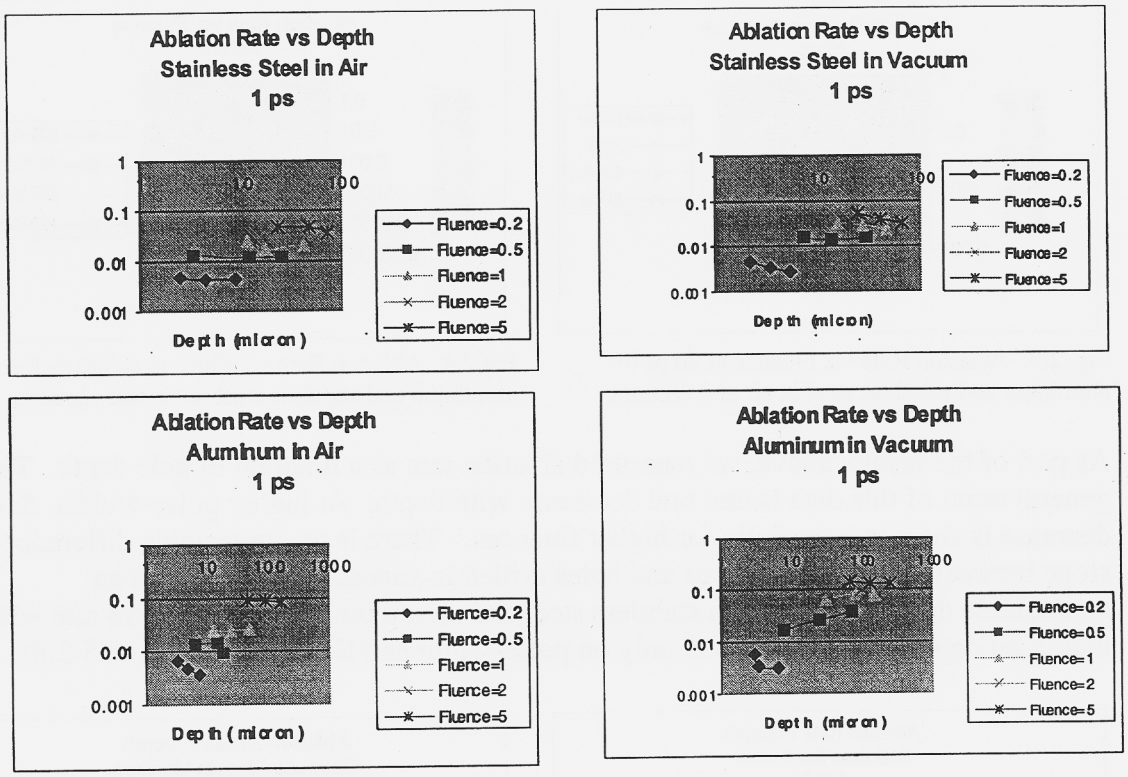

Figure 2.6 Ablation rate vs. hole depth at 1 ps for aluminum and stainless steel in air and vacuum.

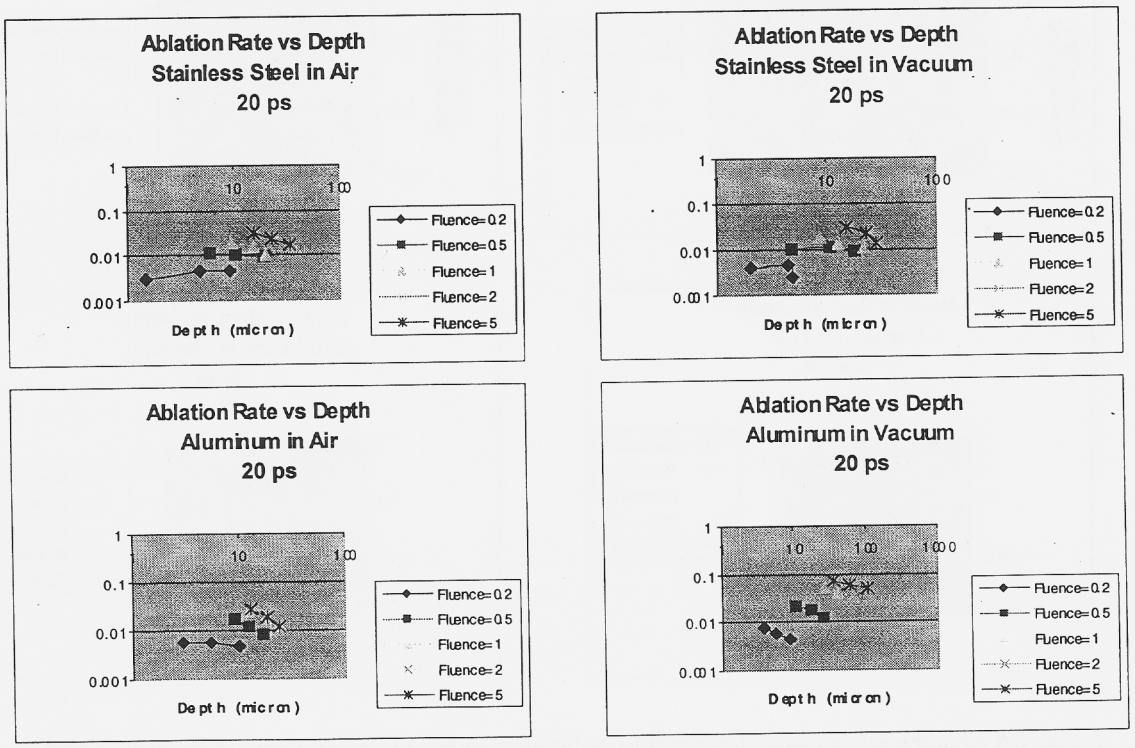

Figure 2.7 Ablation rate vs. hole depth at 20 ps for aluminum and stainless steel in air and vacuum.

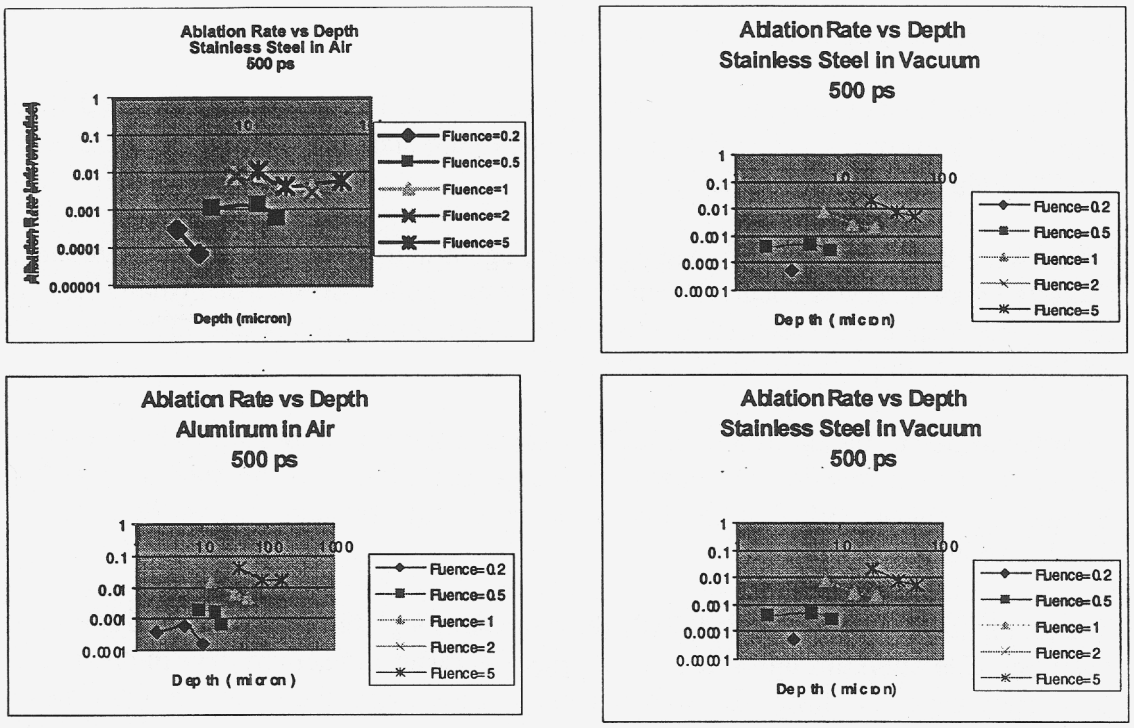

Figure 2.8 Ablation rate vs. hole depth at 500 ps for aluminum and stainless steel in air and vacuum.

2.4 Through-hole drilling in air vs. vacuum

A study was done evaluating break-through times at different pulse-widths and fluences in air and in vacuum. The materials were again 304 stainless steel (900 microns thick) and 7075 aluminum (1 mm thick).

Holes were drilled at 3 J/cm^2, and 15 J/cm^2, again at 1 kHz. At the lower fluence, the Gaussian spot size was focused with an f=64 cm lens to 400 microns (diameter) and at the higher fluence, the Gaussian spot size was 200 microns (diameter). The pulse widths studied were 0.15 ps, 1 ps, 20 ps, and 500 ps.

In order to detect breakthrough, a CCD camera was set up outside the back end of the chamber with a system of lenses to image the plane of the part being drilled. Breakthrough was marked at the time when laser light first appeared on the camera after the shutter was opened.

The graphs below (Figs. 2.9 and 2.10) show breakthrough time vs. pulse-width for air and vacuum. The breakthrough times were generally faster in vacuum than in air (see Table 2.1). They were also faster for higher fluence. In vacuum, the breakthrough times were faster for aluminum in both fluence cases. In air, at 3 J/cm^2, there was no breakthrough detected for aluminum for all but 0.15 ps. We believe that oxidation created a layer with higher ablation threshold than bare aluminum. At 15 J/cm^2, the breakthrough times for stainless steel were faster than aluminum.

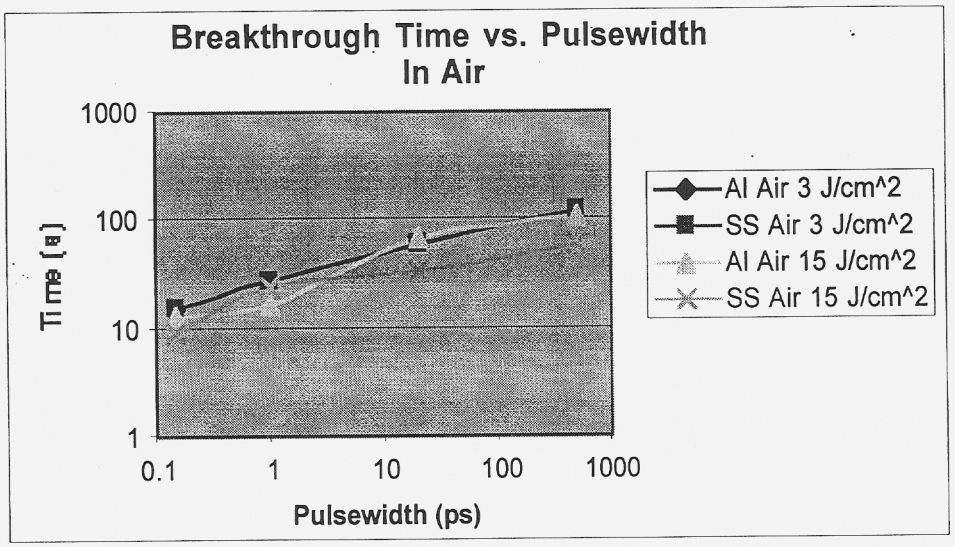

Figure 2.9. Breakthrough time vs. pulse duration in air for aluminum and stainless steel.

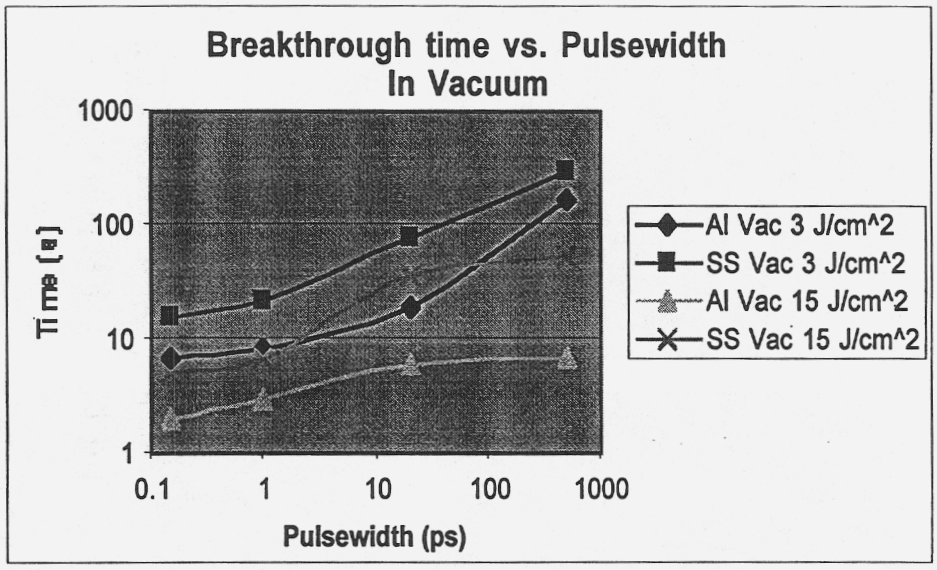

Figure 2.10. Breakthrough time vs. pulse duration in vacuum for aluminum and stainless steel..

PulseWidth	Al Vac 3 J/cm^2	SS Vac 3 J/cm^2	Al Vac 15 J/cm^2	SS Vac 15 J/cm^2
0.15 ps	7 s	16 s	2 s	5 s
1 ps	8 s	22 s	3 s	7 s
20 ps	19 s	75 s	6 s	35 s
500 ps	170 s	294 s	7 s	53 s
PulseWidth	Al Air 3 J/cm^2	SS Air 3 J/cm^2	Al Air 15 J/cm^2	SS Air 15 J/cm^2
0.15 ps	15 s	15 s	13 s	9 s
1 ps	–	28 s	17 s	25 s
20 ps	–	62 s	70 s	33 s
500 ps	–	124 s	108 s	59 s

Table 2.1. Breakthrough times measured at various pulse durations and fluences for 1-mm thick aluminum and 0.9-mm thick stainless steel.

The presence or absence of air also affects the hole shape and quality. Pictures of the entrance and exit surfaces are presented below (Figure 2.11). The holes were drilled to breakthrough (brk) and cleaned out by drilling to five times the breakthrough time (5brk).

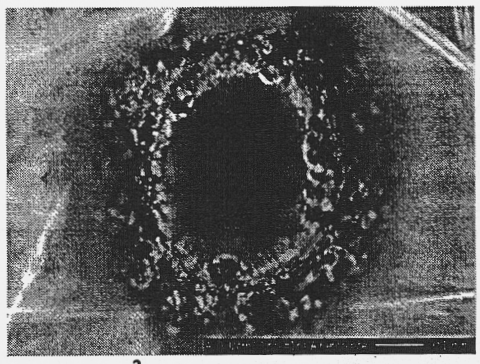

Air: 3 J/cm^2, brk=15s, entrance

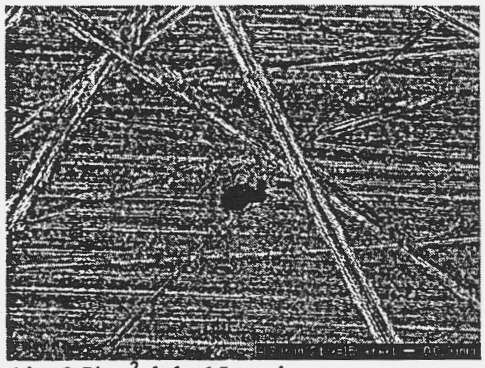

Air: 3 J/cm^2, brk=15s, exit

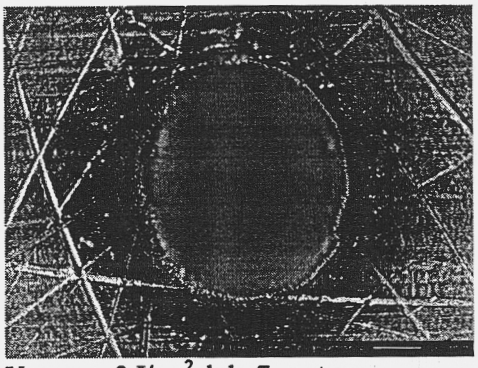

Vacuum: 3 J/cm^2, brk=7s, entrance

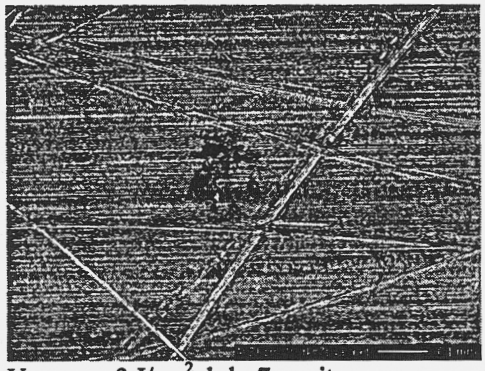

Vacuum: 3 J/cm^2, brk=7s, exit

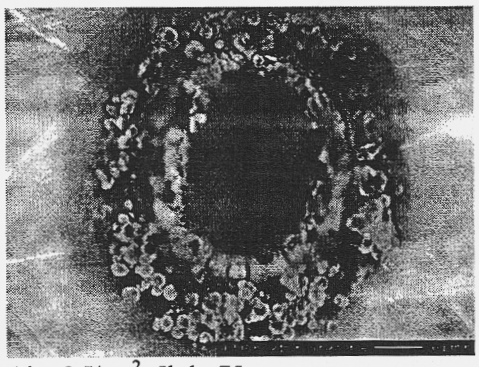

Air: 3 J/cm^2, 5brk=75s, entrance

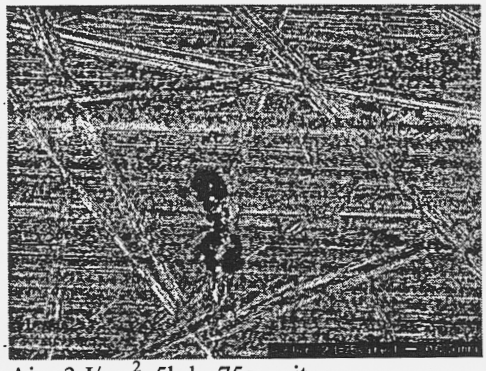

Air: 3 J/cm^2, 5brk=75s, exit

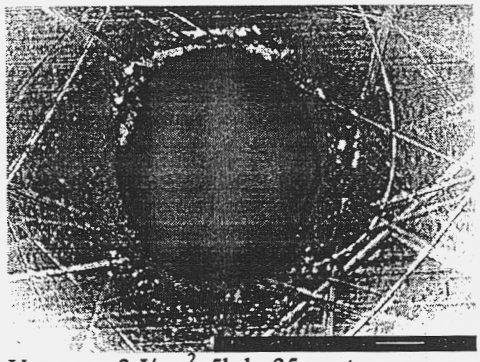

Vacuum: 3 J/cm^2, 5brk=35s, entrance

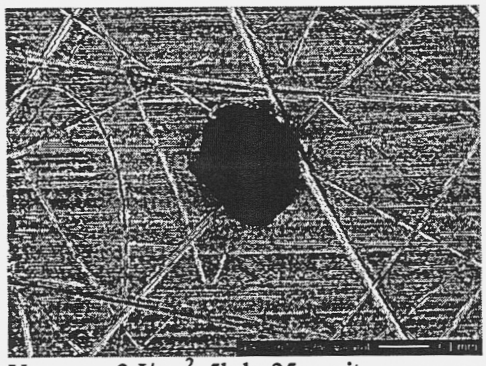

Vacuum: 3 J/cm^2, 5brk=35s, exit

Figure 2.11a. Entrance and exit surfaces of holes drilled by 150-fs, 400-μm diameter laser spot on 1-mm thick 7075 aluminum at a fluence of 3 J/cm^2, showing the difference in shape and quality of holes drilled in vacuum and air.

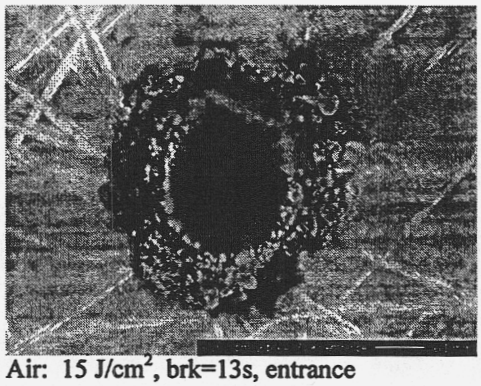

Air: 15 J/cm^2, brk=13s, entrance

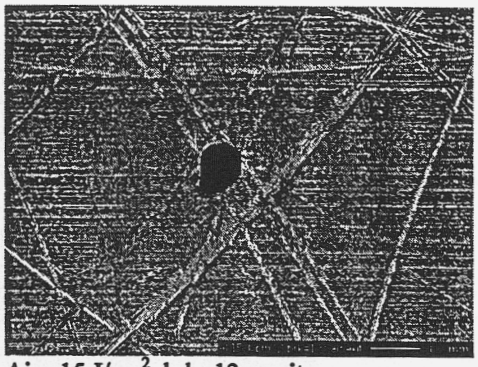

Air: 15 J/cm^2, brk=13s, exit

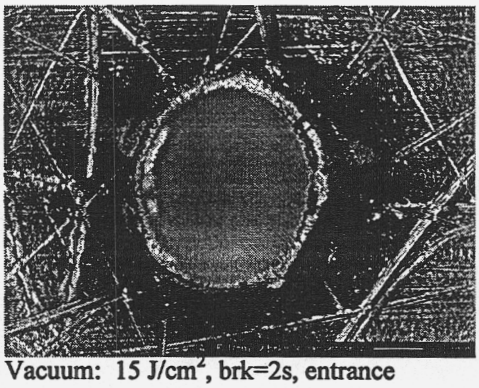

Vacuum: 15 J/cm^2, brk=2s, entrance

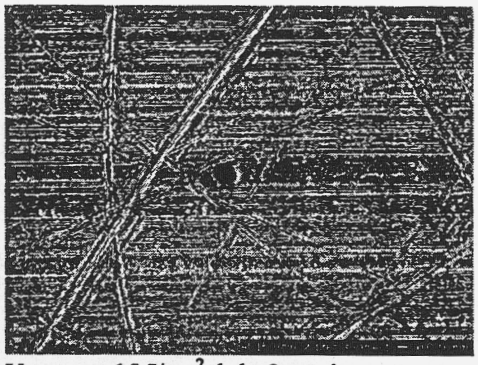

Vacuum: 15 J/cm^2, brk=2s, exit

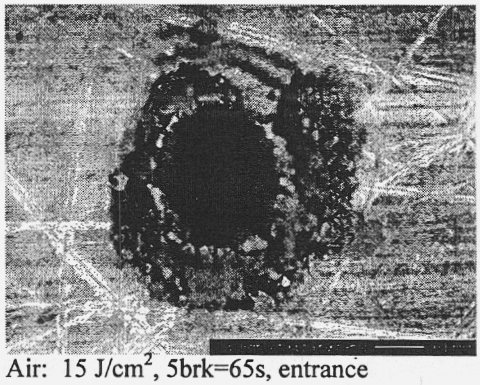

Air: 15 J/cm^2, 5brk=65s, entrance

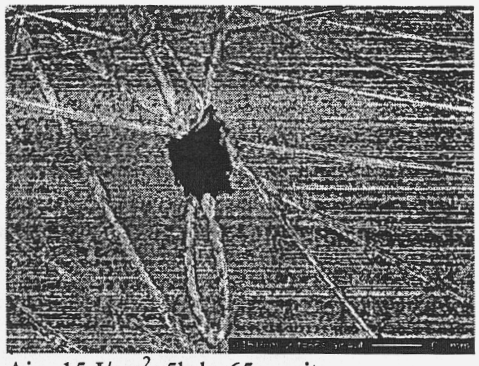

Air: 15 J/cm^2, 5brk=65s, exit

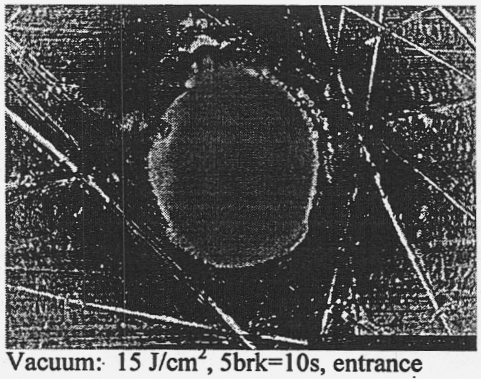

Vacuum: 15 J/cm^2, 5brk=10s, entrance

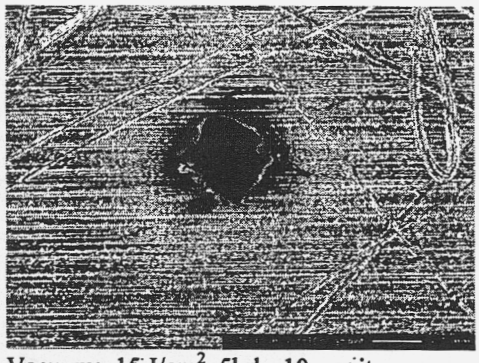

Vacuum: 15 J/cm^2, 5brk=10s, exit

Figure 2.11b: Entrance and exit surfaces of holes drilled by 150-fs, 200-μm diameter laser spot on 1-mm thick 7075 aluminum at a fluence of 15 J/cm^2, showing the difference in shape and quality of holes drilled in vacuum and air.

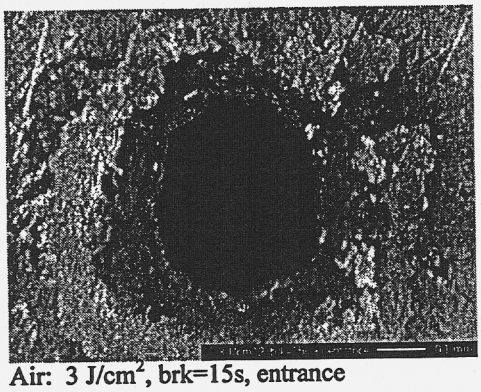

Air: 3 J/cm^2, brk=15s, entrance

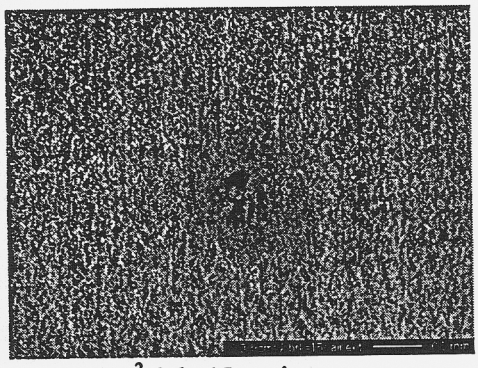

Air: 3 J/cm^2, brk=15s, exit

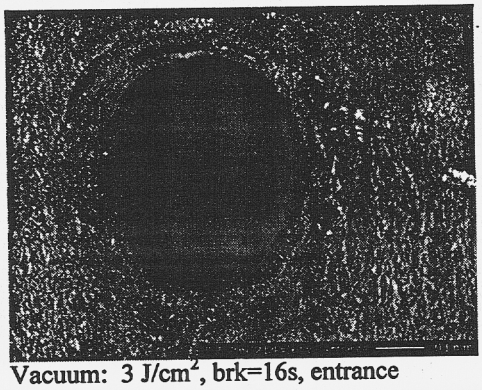

Vacuum: 3 J/cm^2, brk=16s, entrance

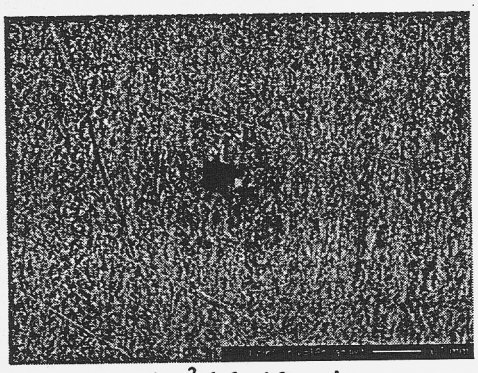

Vacuum: 3 J/cm^2, brk=16s, exit

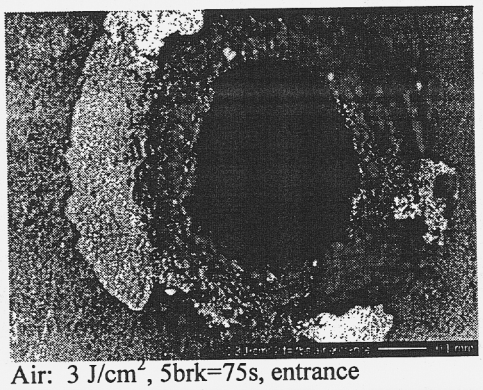

Air: 3 J/cm^2, 5brk=75s, entrance

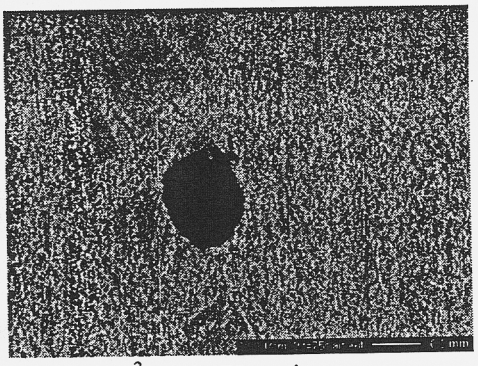

Air: 3 J/cm^2, 5brk=75s, exit

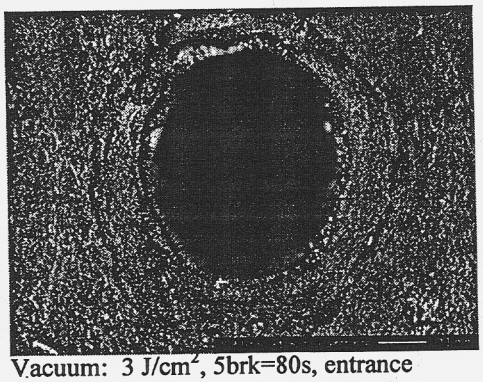

Vacuum: 3 J/cm^2, 5brk=80s, entrance

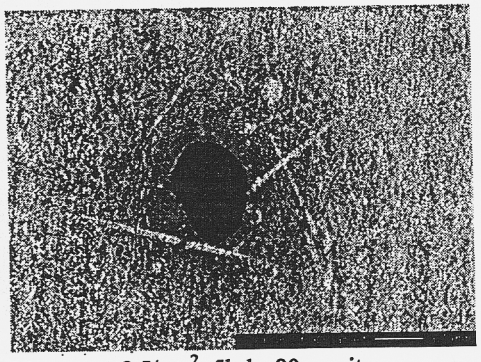

Vacuum: 3 J/cm^2, 5brk=80s, exit

Figure 2.11c. Entrance and exit surfaces of holes drilled by 150-fs, 400-μm diameter laser spot on 0.9-mm thick 304 stainless steel at a fluence of 3 J/cm^2, showing the difference in shape and quality of holes drilled in vacuum and air.

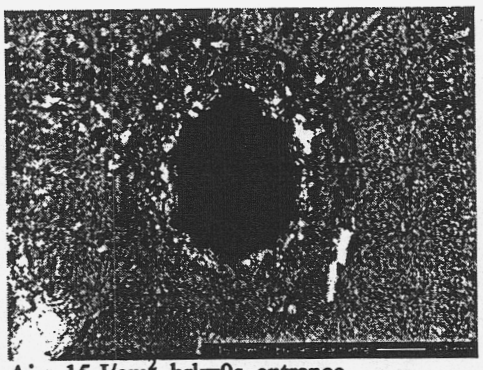

Air: 15 J/cm^2, brk=9s, entrance

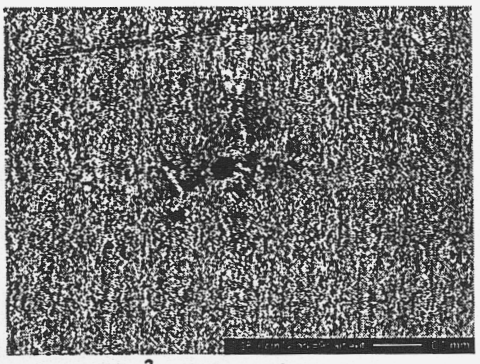

Air: 15 J/cm^2, brk=9s, exit

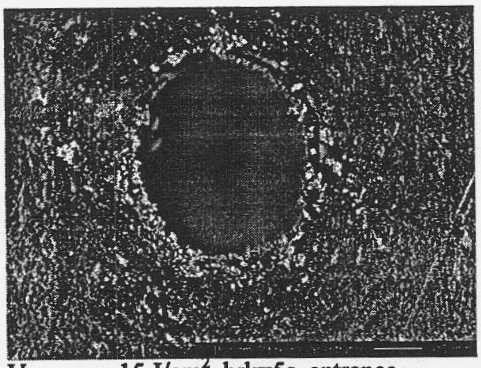

Vacuum: 15 J/cm^2, brk=5s, entrance

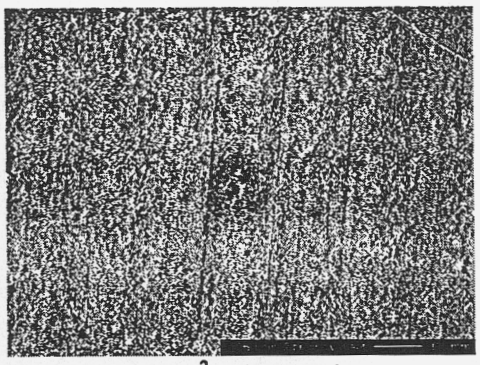

Vacuum: 15 J/cm^2, brk=5s, exit

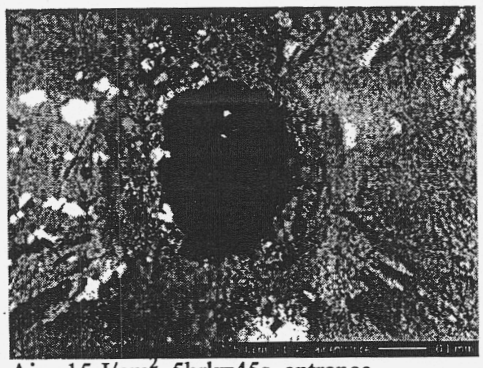

Air: 15 J/cm^2, 5brk=45s, entrance

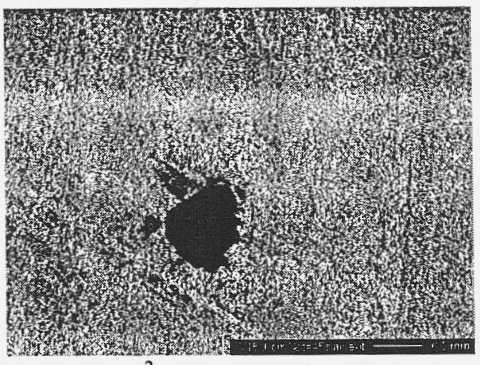

Air: 15 J/cm^2, 5brk=45s, exit

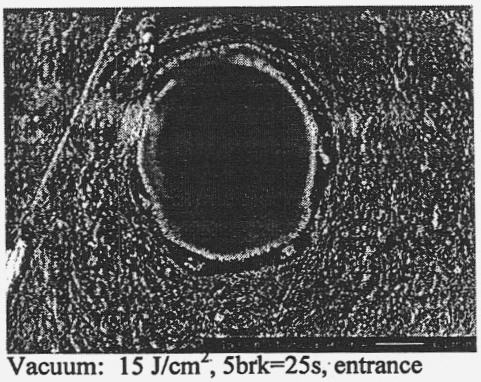

Vacuum: 15 J/cm^2, 5brk=25s, entrance

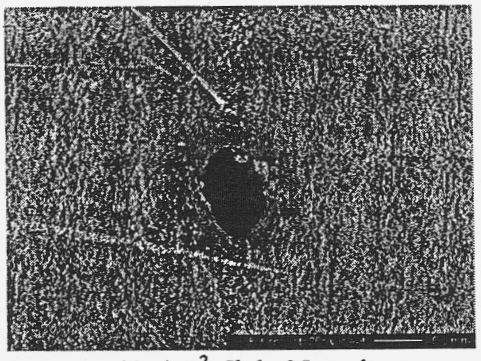

Vacuum: 15 J/cm^2, 5brk=25s, exit

Figure 2.11d. Entrance and exit surfaces of holes drilled by 150-fs, 200-μm diameter laser spot on 0.9-mm thick 304 stainless steel at a fluence of 15 J/cm^2, showing the difference in shape and quality of holes drilled in vacuum and air.

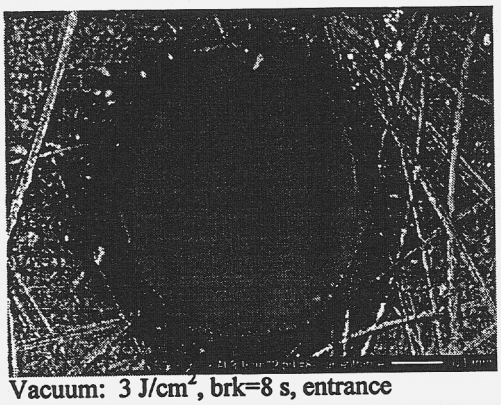

Vacuum: 3 J/cm^2, brk=8 s, entrance

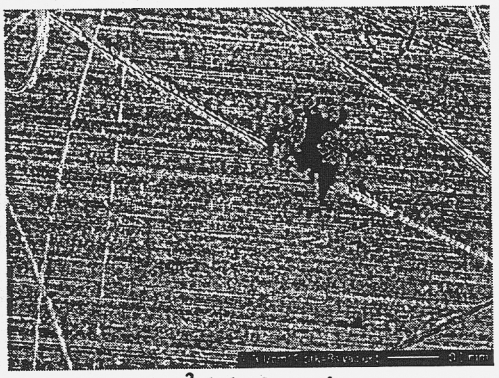

Vacuum: 3 J/cm^2, brk=8 s, exit

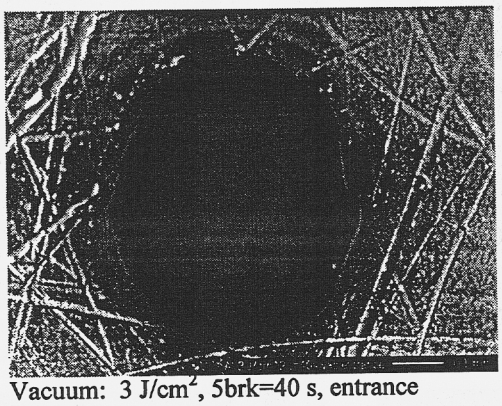

Vacuum: 3 J/cm^2, 5brk=40 s, entrance

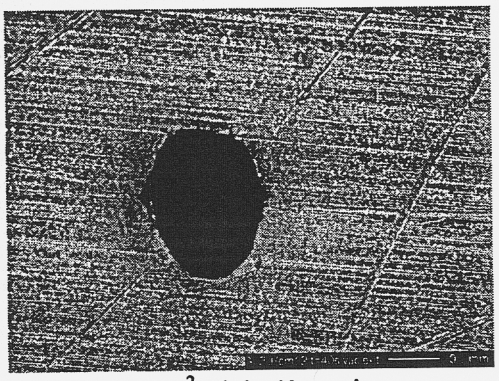

Vacuum: 3 J/cm^2, 5brk=40 s, exit

Figure 2.11e. Entrance and exit surfaces of holes drilled by 1-ps, 400-μm diameter laser spot on 1-mm thick 7075 aluminum at a fluence of 3 J/cm^2, showing the difference in shape and quality of holes drilled in vacuum. The holes drilled in air at this fluence and pulse duration did not break through.

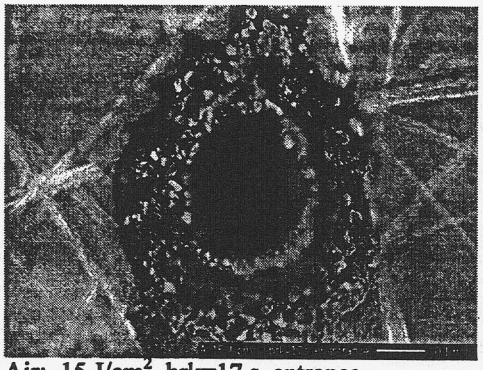

Air: 15 J/cm^2, brk=17 s, entrance

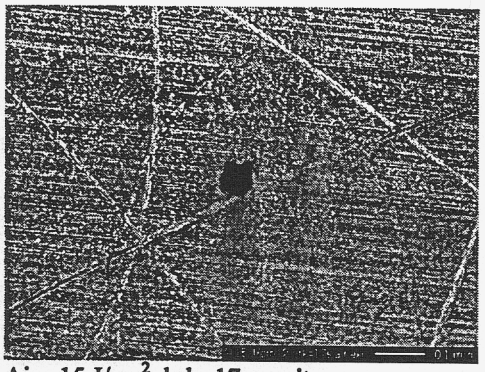

Air: 15 J/cm^2, brk=17 s, exit

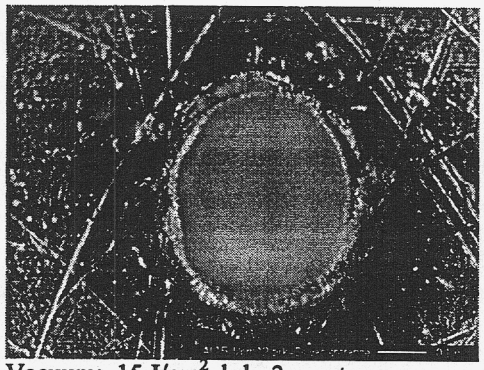

Vacuum: 15 J/cm^2, brk=3 s, entrance

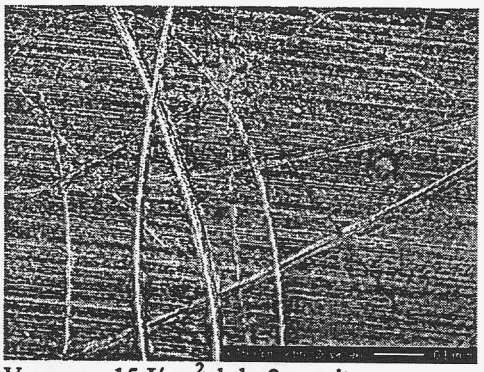

Vacuum: 15 J/cm^2, brk=3 s, exit

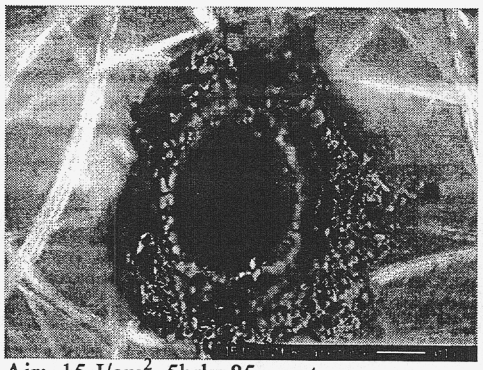

Air: 15 J/cm^2, 5brk=85 s, entrance

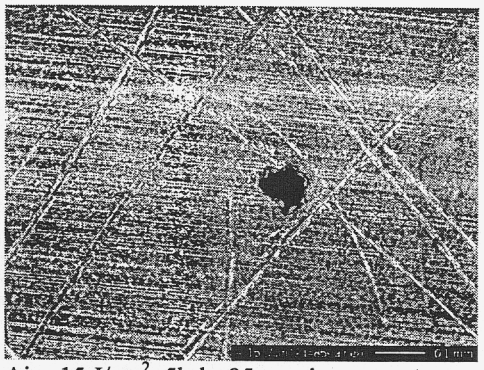

Air: 15 J/cm^2, 5brk=85 s, exit

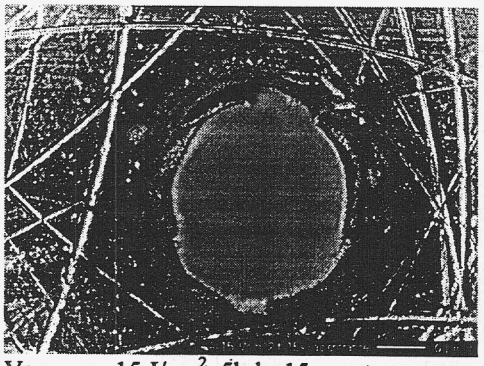

Vacuum: 15 J/cm^2, 5brk=15 s, entrance

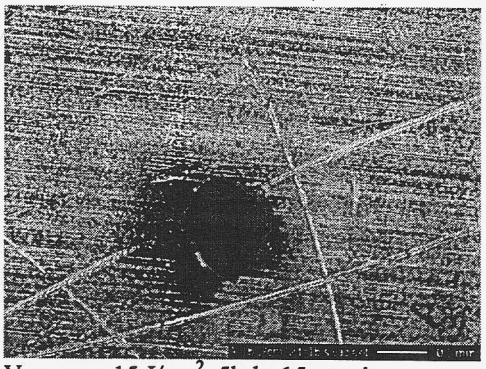

Vacuum: 15 J/cm^2, 5brk=15 s, exit

Figure 2.11f. Entrance and exit surfaces of holes drilled by 1-ps, 200-μm diameter laser spot on 1-mm thick 7075 aluminum at a fluence of 15 J/cm^2, showing the difference in shape and quality of holes drilled in vacuum and air.

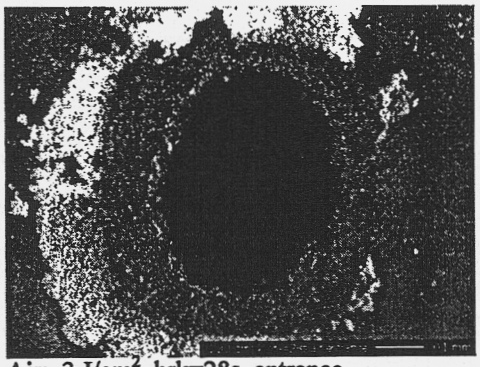

Air: 3 J/cm^2, brk=28s, entrance

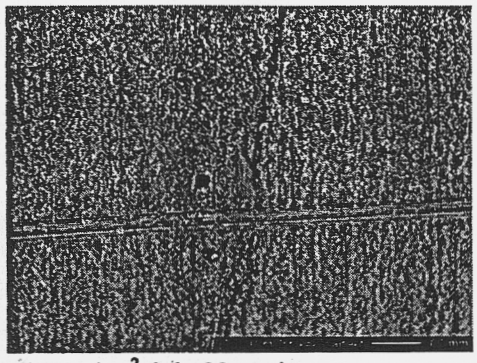

Air: 3 J/cm^2, brk=28s, exit

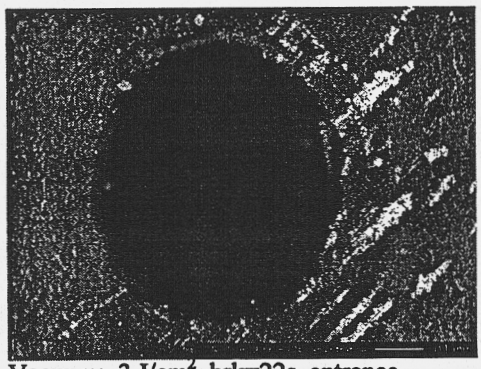

Vacuum: 3 J/cm^2, brk=22s, entrance

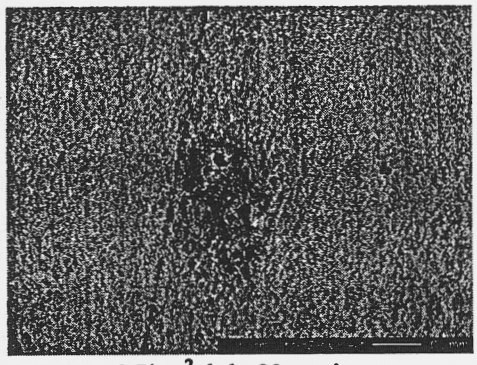

Vacuum: 3 J/cm^2, brk=22s, exit

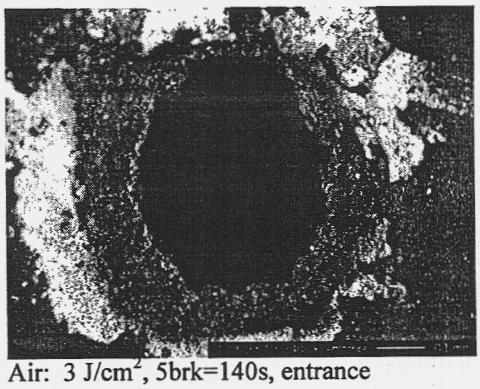

Air: 3 J/cm^2, 5brk=140s, entrance

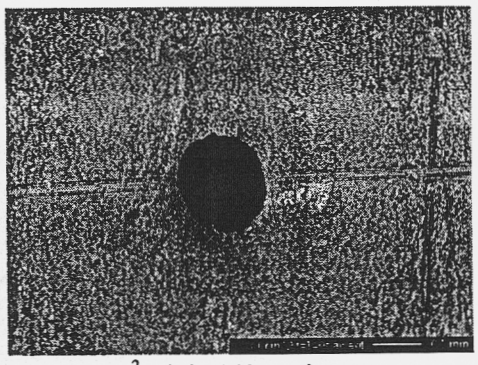

Air: 3 J/cm^2, 5brk=140s, exit

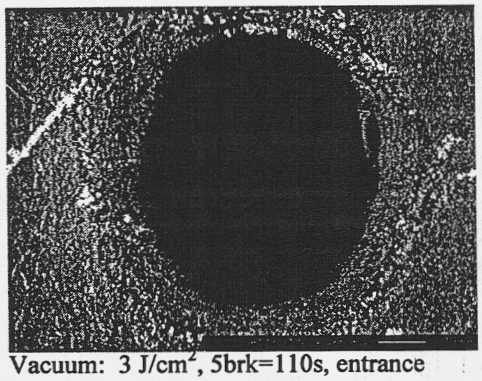

Vacuum: 3 J/cm^2, 5brk=110s, entrance

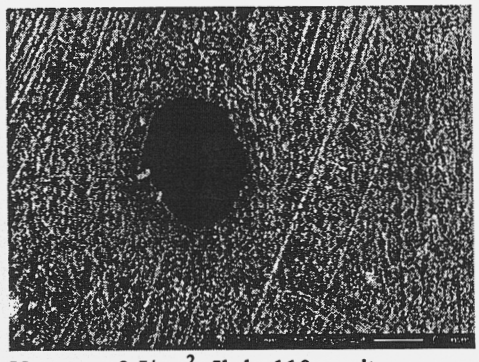

Vacuum: 3 J/cm^2, 5brk=110s, exit

Figure 2.11g. Entrance and exit surfaces of holes drilled by 1-ps, 400-μm diameter laser spot on 0.9-mm thick 304 stainless steel at a fluence of 3 J/cm^2, showing the difference in shape and quality of holes drilled in vacuum and air.

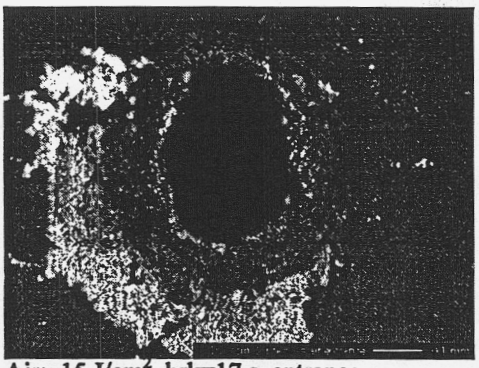

Air: 15 J/cm^2, brk=17 s, entrance

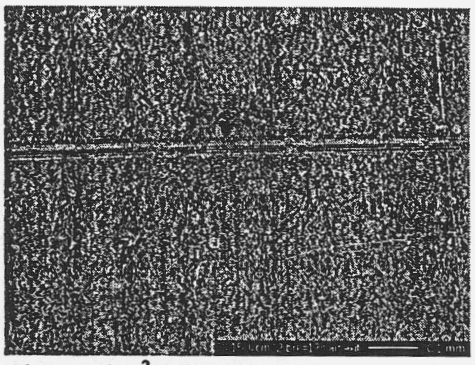

Air: 15 J/cm^2, brk=17 s, exit

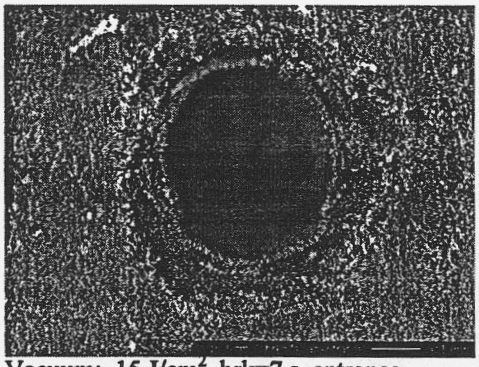

Vacuum: 15 J/cm^2, brk=7 s, entrance

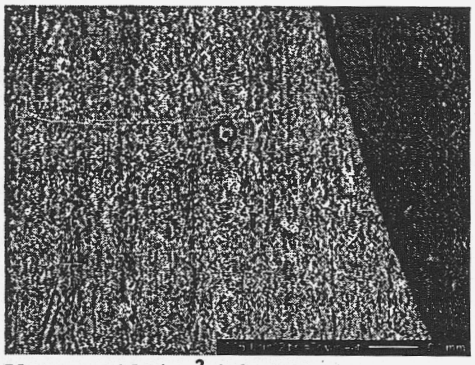

Vacuum: 15 J/cm^2, brk=7 s, exit

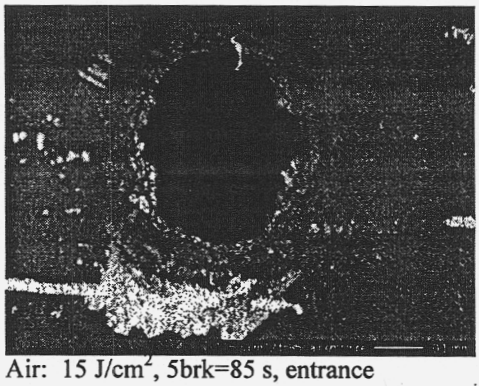

Air: 15 J/cm^2, 5brk=85 s, entrance

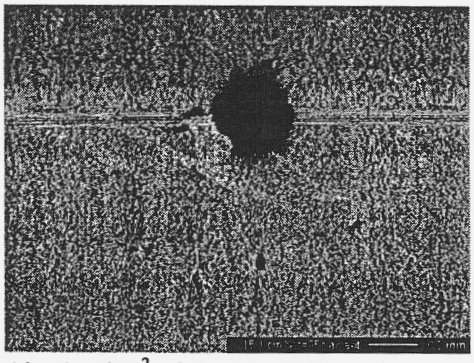

Air: 15 J/cm^2, 5brk=85 s, exit

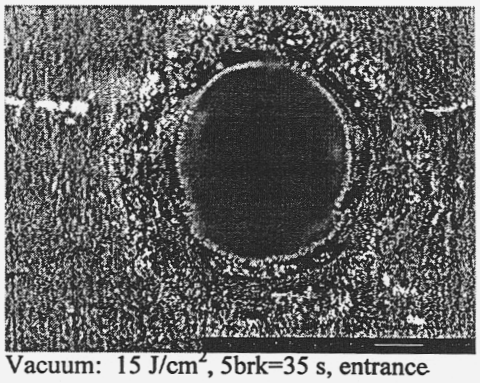

Vacuum: 15 J/cm^2, 5brk=35 s, entrance

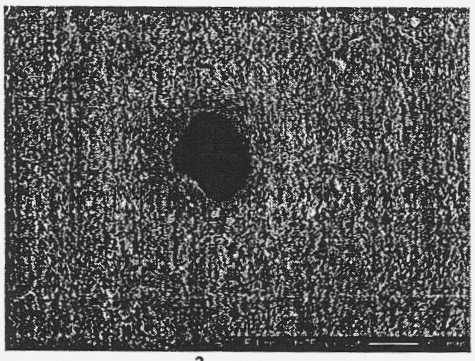

Vacuum: 15 J/cm^2, 5brk=35 s, exit

Figure 2.11h. Entrance and exit surfaces of holes drilled by 1-ps, 200-μm diameter laser spot on 0.9-mm thick 304 stainless steel at a fluence of 15 J/cm^2, showing the difference in shape and quality of holes drilled in vacuum and air.

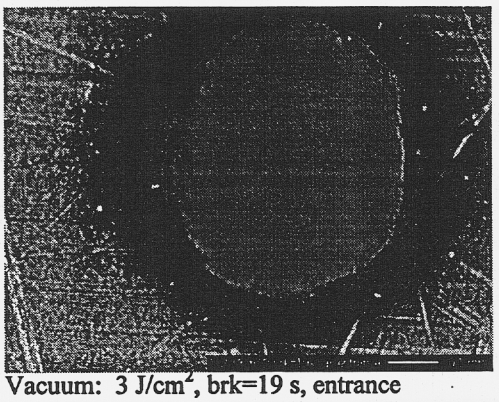

Vacuum: 3 J/cm^2, brk=19 s, entrance

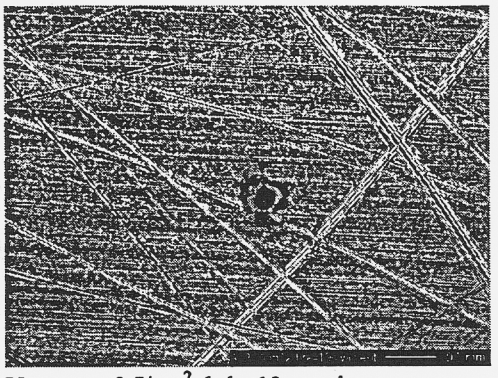

Vacuum: 3 J/cm^2, brk=19 s, exit

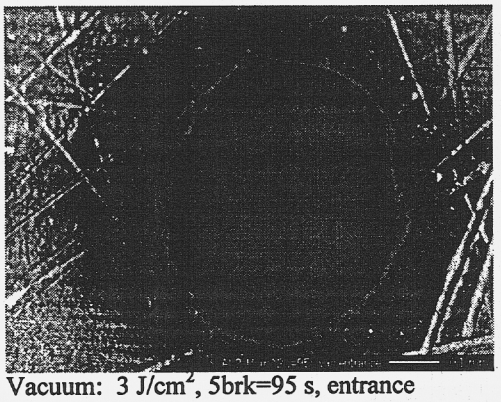

Vacuum: 3 J/cm^2, 5brk=95 s, entrance

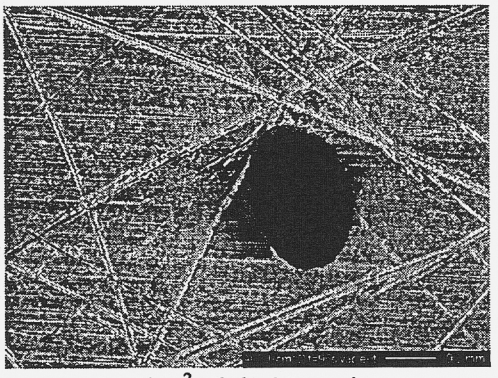

Vacuum: 3 J/cm^2, 5brk=95 s, exit

Figure 2.11i. Entrance and exit surfaces of holes drilled by 20-ps, 400-μm diameter laser spot on 1-mm thick 7075 aluminum at a fluence of 3 J/cm^2, showing the difference in shape and quality of holes drilled in vacuum. The holes drilled in air at this fluence and pulse duration did not break through.

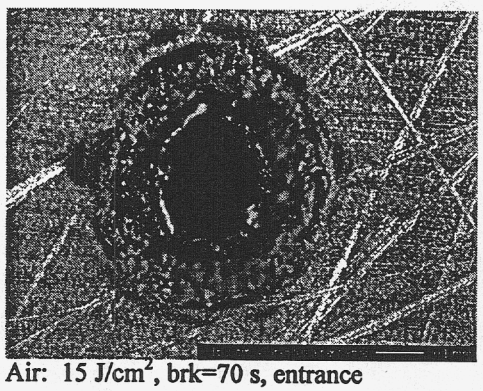

Air: 15 J/cm^2, brk=70 s, entrance

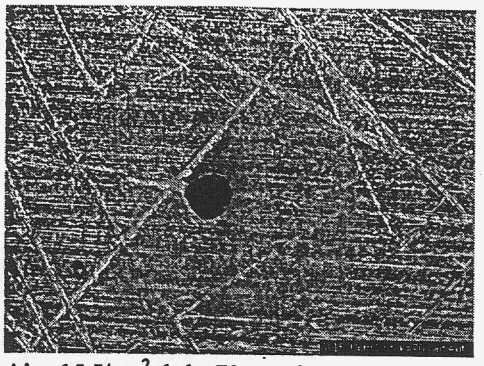

Air: 15 J/cm^2, brk=70 s, exit

Vacuum: 15 J/cm^2, brk=6 s, entrance

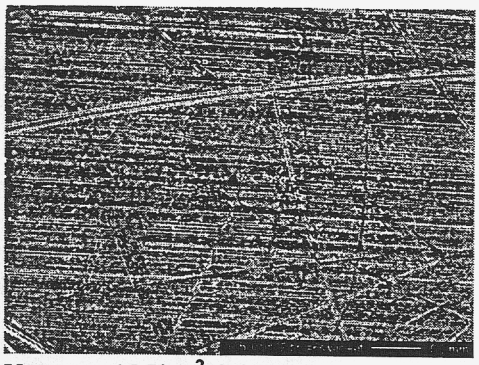

Vacuum: 15 J/cm^2, brk=6 s, exit

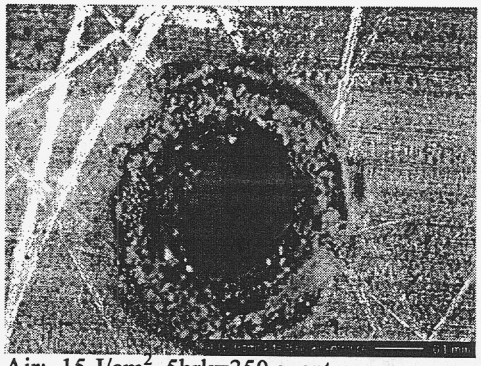

Air: 15 J/cm^2, 5brk=350 s, entrance

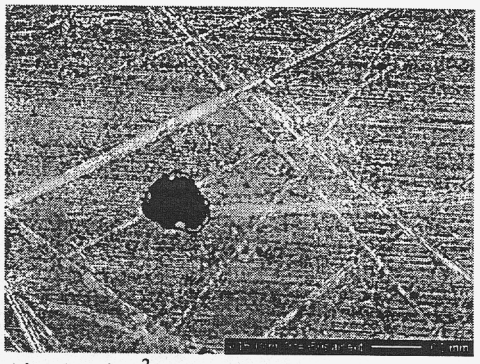

Air: 15 J/cm^2, 5brk=350 s, exit

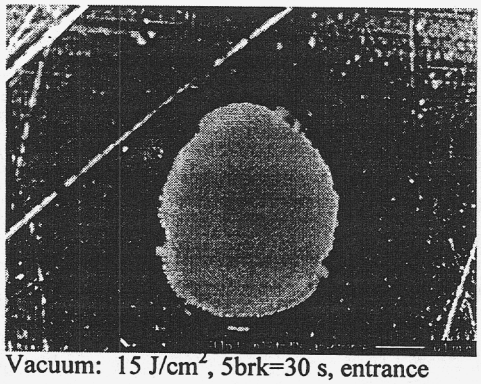

Vacuum: 15 J/cm^2, 5brk=30 s, entrance

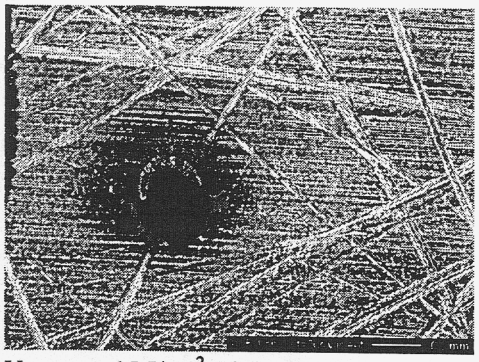

Vacuum: 15 J/cm^2, 5brk=30 s, exit

Figure 2.11j. Entrance and exit surfaces of holes drilled by 20-ps, 200-μm diameter laser spot on 1-mm thick 7075 aluminum at a fluence of 15 J/cm^2, showing the difference in shape and quality of holes drilled in vacuum and air.

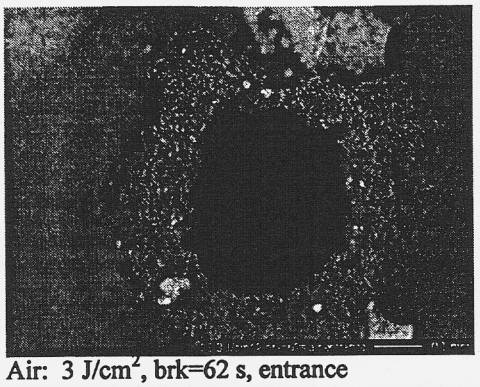

Air: 3 J/cm^2, brk=62 s, entrance

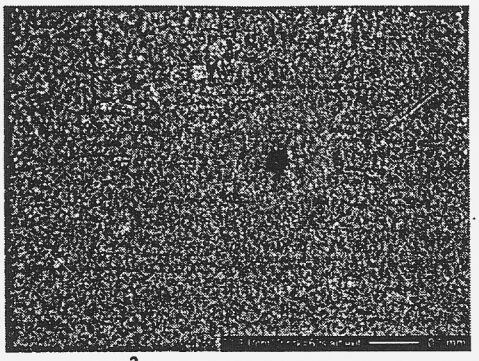

Air: 3 J/cm^2, brk=62 s, exit

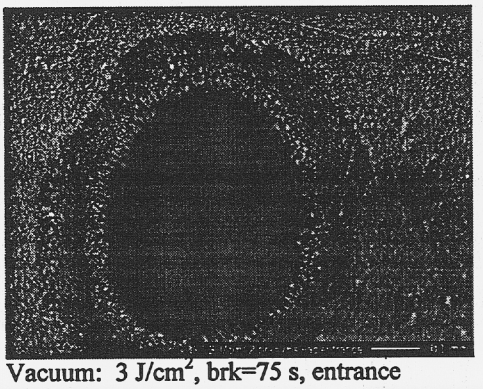

Vacuum: 3 J/cm^2, brk=75 s, entrance

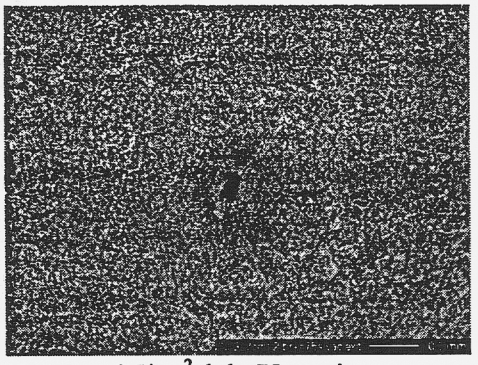

Vacuum: 3 J/cm^2, brk=75 s, exit

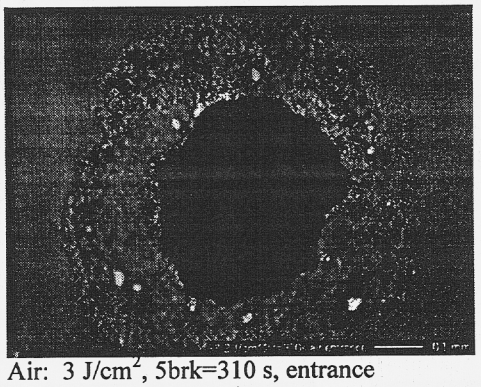

Air: 3 J/cm^2, 5brk=310 s, entrance

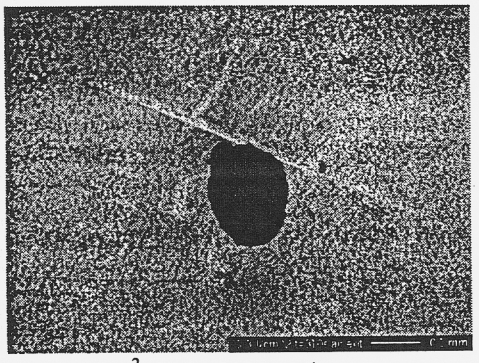

Air: 3 J/cm^2, 5brk=310 s, exit

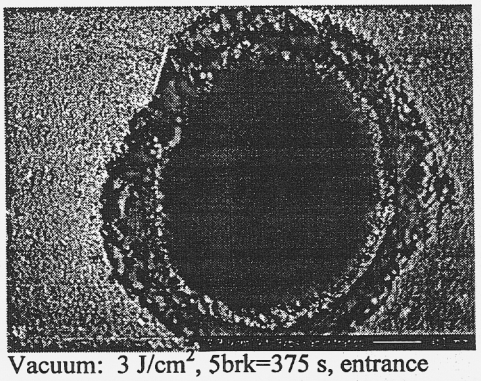

Vacuum: 3 J/cm^2, 5brk=375 s, entrance

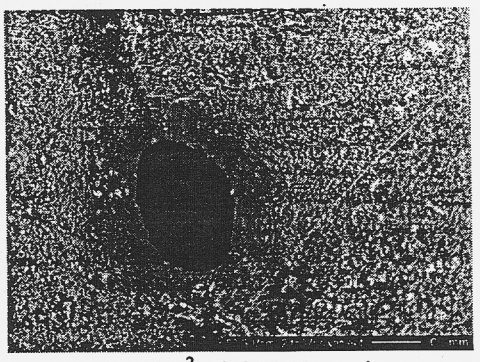

Vacuum: 3 J/cm^2, 5brk=375 s, exit

Figure 2.11k. Entrance and exit surfaces of holes drilled by 20-ps, 400-μm diameter laser spot on 0.9-mm thick 304 stainless steel at a fluence of 3 J/cm^2, showing the difference in shape and quality of holes drilled in vacuum and air.

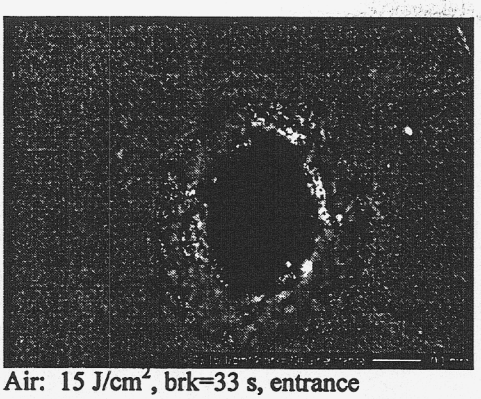

Air: 15 J/cm^2, brk=33 s, entrance

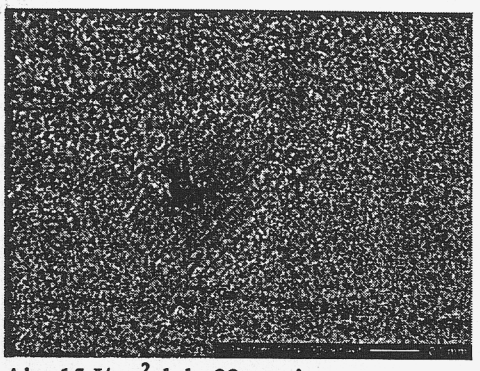

Air: 15 J/cm^2, brk=33 s, exit

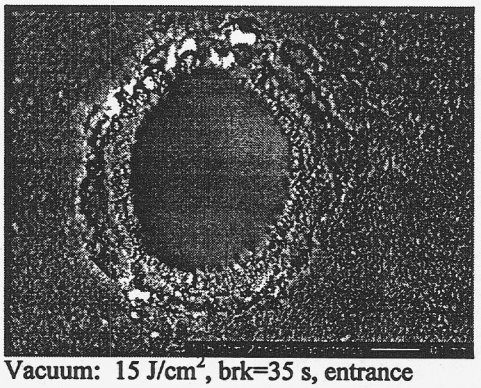

Vacuum: 15 J/cm^2, brk=35 s, entrance

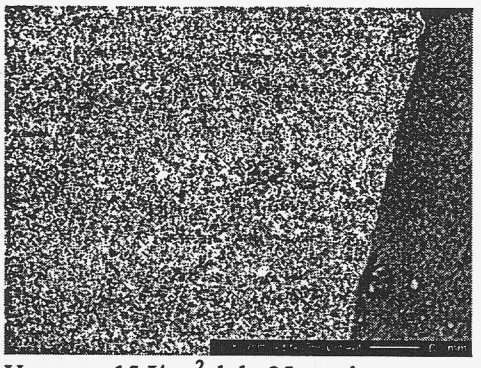

Vacuum: 15 J/cm^2, brk=35 s, exit

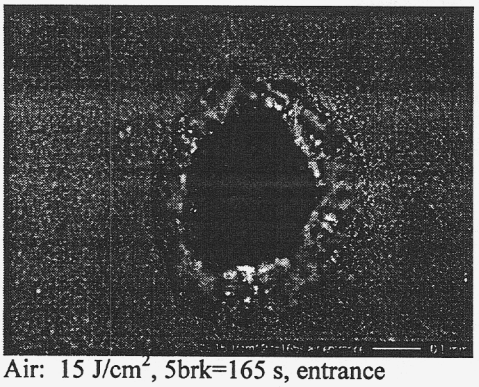

Air: 15 J/cm^2, 5brk=165 s, entrance

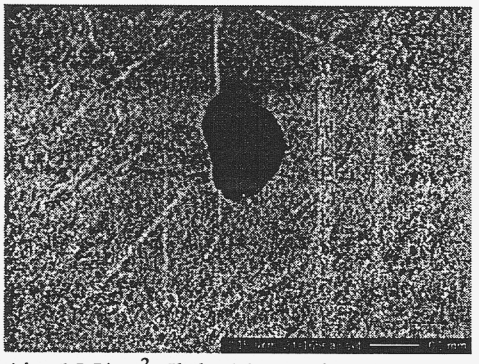

Air: 15 J/cm^2, 5brk=165 s, exit

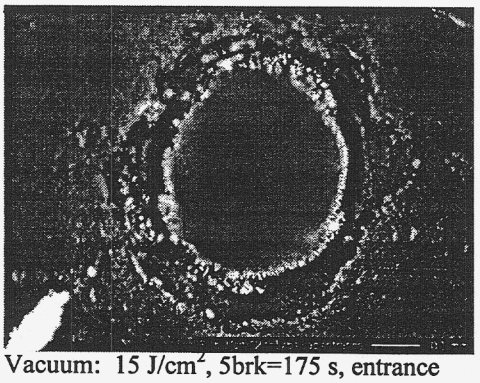

Vacuum: 15 J/cm^2, 5brk=175 s, entrance

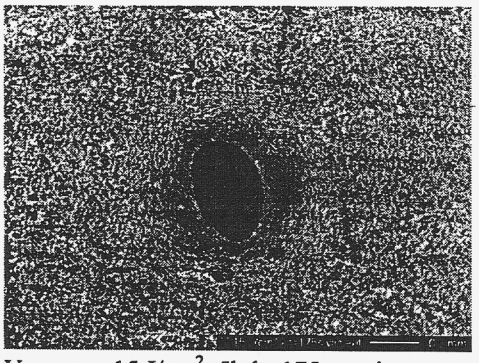

Vacuum: 15 J/cm^2, 5brk=175 s, exit

Figure 2.111. Entrance and exit surfaces of holes drilled by 20-ps, 200-μm diameter laser spot on 0.9-mm thick 304 stainless steel at a fluence of 15 J/cm^2, showing the difference in shape and quality of holes drilled in vacuum and air.

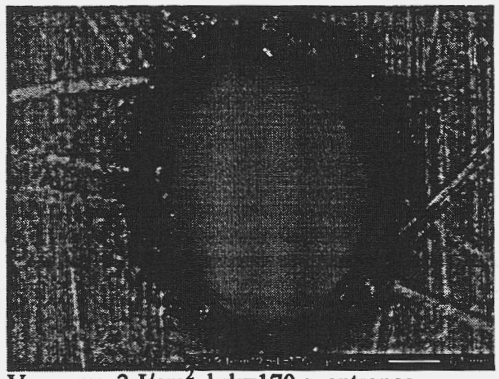

Vacuum: 3 J/cm^2, brk=170 s, entrance

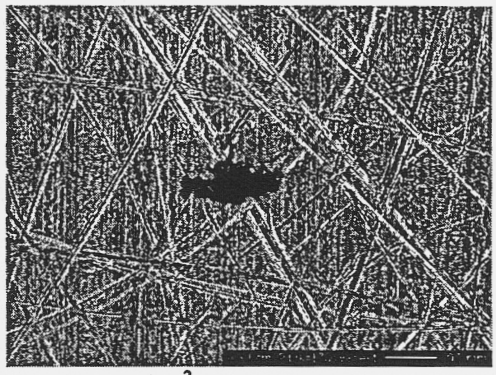

Vacuum: 3 J/cm^2, brk=170 s, exit

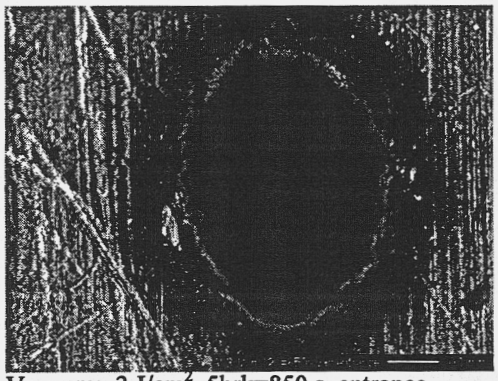

Vacuum: 3 J/cm^2, 5brk=850 s, entrance

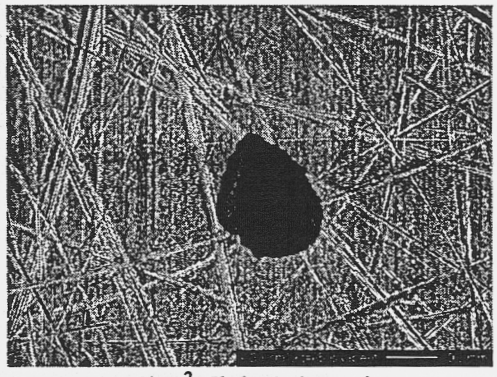

Vacuum: 3 J/cm^2, 5brk=850 s, exit

Figure 2.11m. Entrance and exit surfaces of holes drilled by 500-ps, 400-μm diameter laser spot on 1-mm thick 7075 aluminum at a fluence of 3 J/cm^2, showing the difference in shape and quality of holes drilled in vacuum. The holes drilled in air at this fluence and pulse duration did not break through.

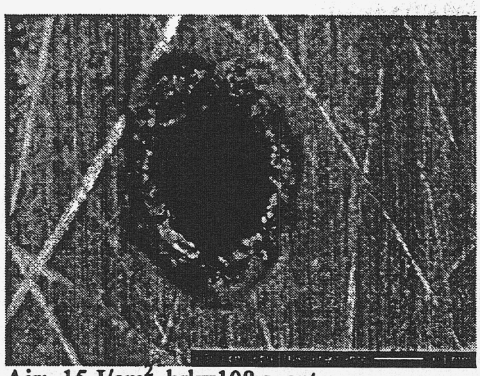

Air: 15 J/cm^2, brk=108 s, entrance

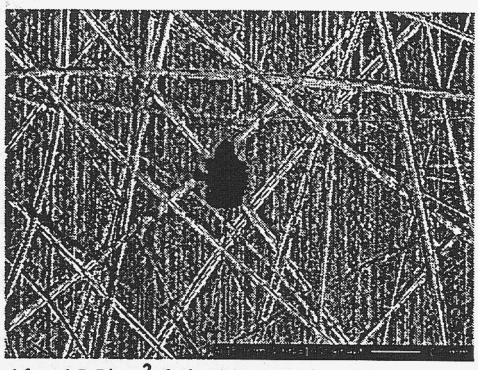

Air: 15 J/cm^2, brk=108 s, exit

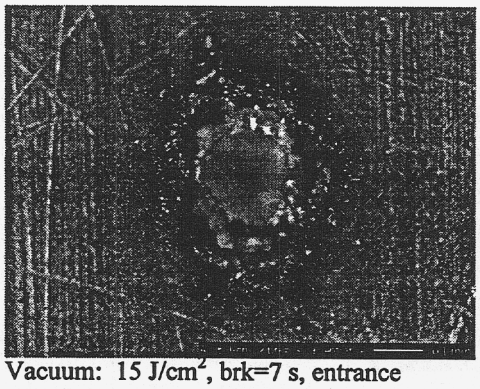

Vacuum: 15 J/cm^2, brk=7 s, entrance

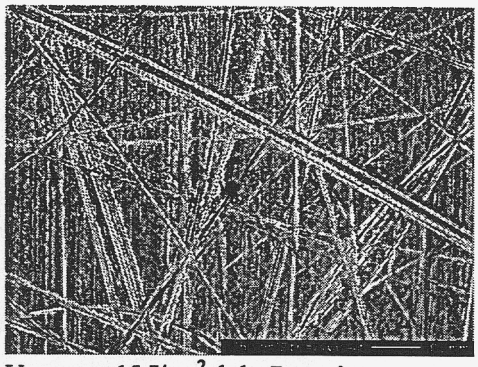

Vacuum: 15 J/cm^2, brk=7 s, exit

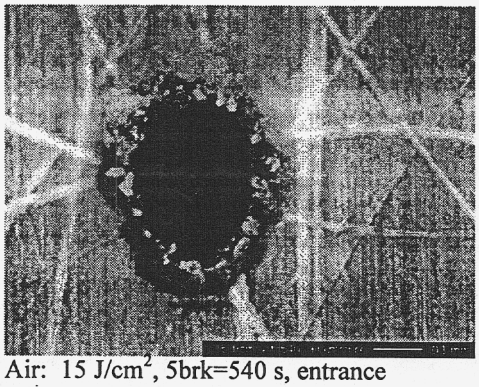

Air: 15 J/cm^2, 5brk=540 s, entrance

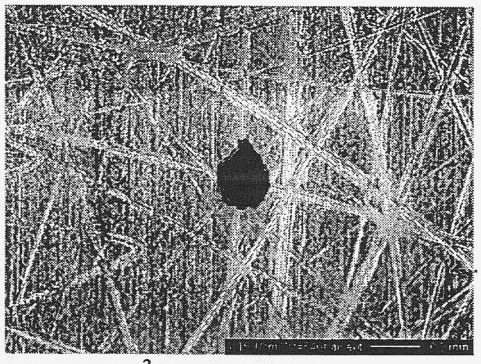

Air: 15 J/cm^2, 5brk=540 s, exit

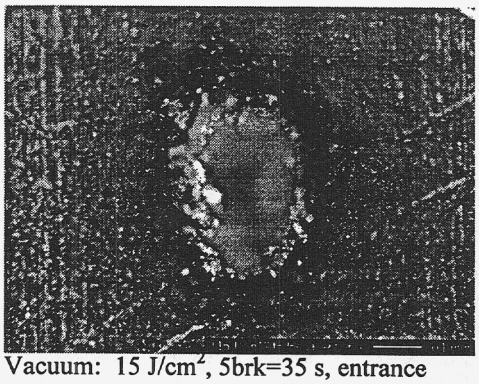

Vacuum: 15 J/cm^2, 5brk=35 s, entrance

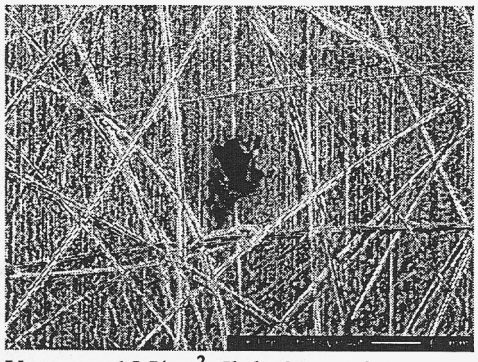

Vacuum: 15 J/cm^2, 5brk=35 s, exit

Figure 2.11n. Entrance and exit surfaces of holes drilled by 20-ps, 200-μm diameter laser spot on 1-mm thick 7075 aluminum at a fluence of 15 J/cm^2, showing the difference in shape and quality of holes drilled in vacuum and air.

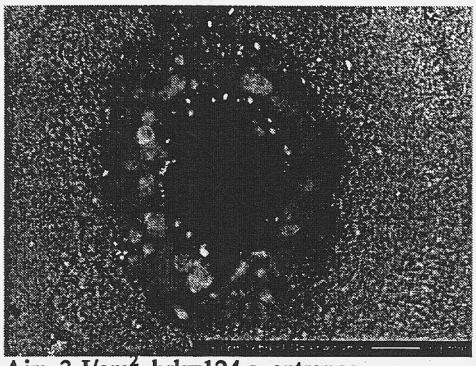

Air: 3 J/cm^2, brk=124 s, entrance

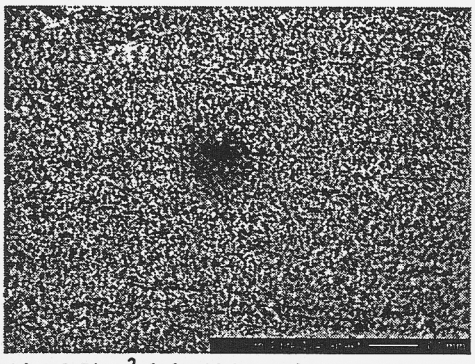

Air: 3 J/cm^2, brk=124 s, exit

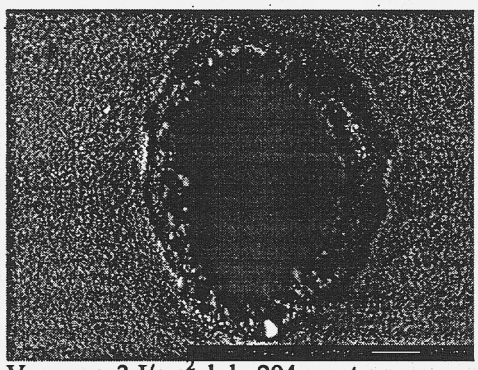

Vacuum: 3 J/cm^2, brk=294 s, entrance

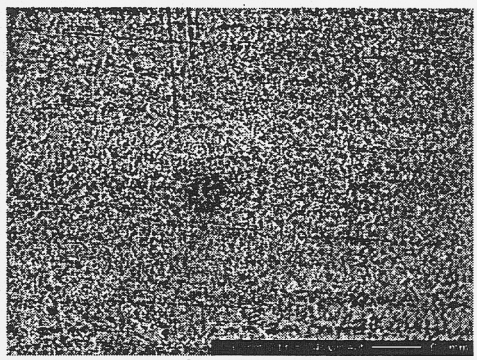

Vacuum: 3 J/cm^2, brk=294 s, exit

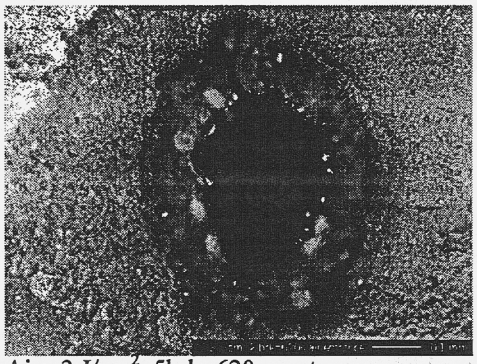

Air: 3 J/cm^2, 5brk=620 s, entrance

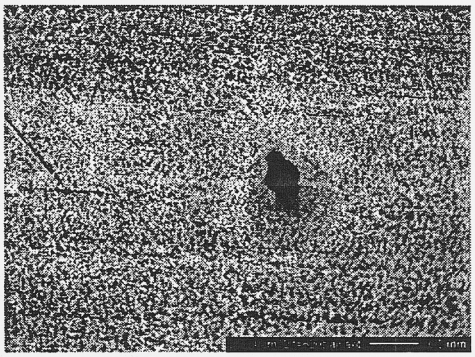

Air: 3 J/cm^2, 5brk=620 s, exit

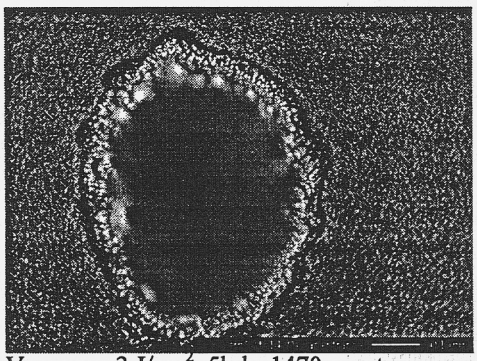

Vacuum: 3 J/cm^2, 5brk=1470 s, entrance

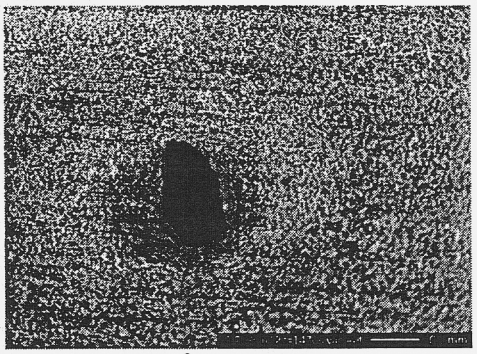

Vacuum: 3 J/cm^2, 5brk=1470 s, exit

Figure 2.11o. Entrance and exit surfaces of holes drilled by 500-ps, 400-μm diameter laser spot on 0.9-mm thick 304 stainless steel at a fluence of 3 J/cm^2, showing the difference in shape and quality of holes drilled in vacuum and air.

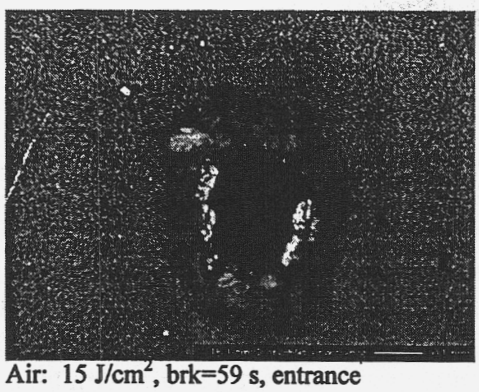

Air: 15 J/cm^2, brk=59 s, entrance

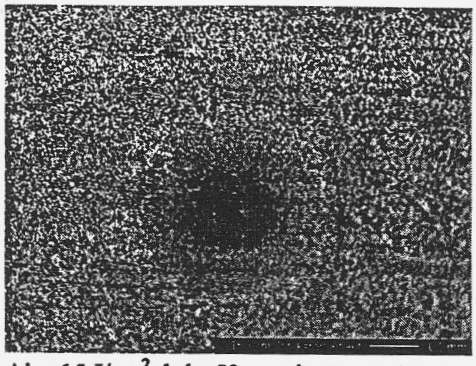

Air: 15 J/cm^2, brk=59 s, exit

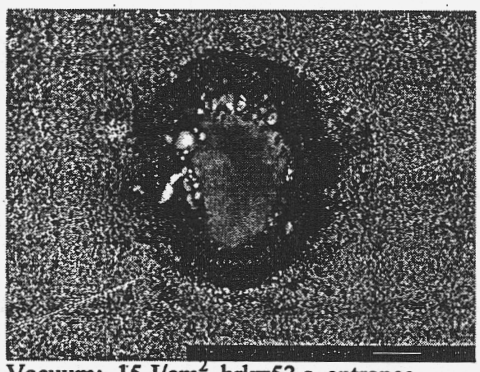

Vacuum: 15 J/cm^2, brk=53 s, entrance

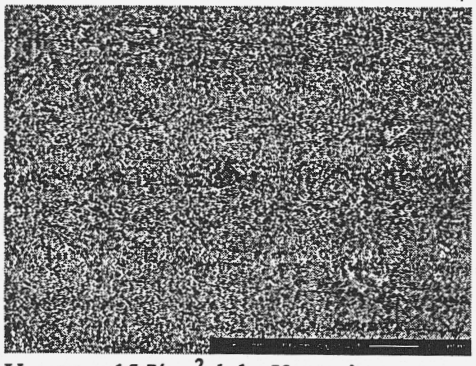

Vacuum: 15 J/cm^2, brk=53 s, exit

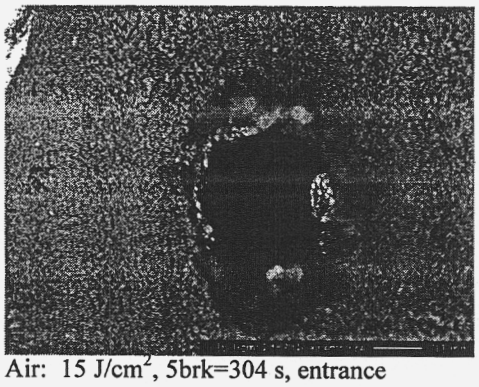

Air: 15 J/cm^2, 5brk=304 s, entrance

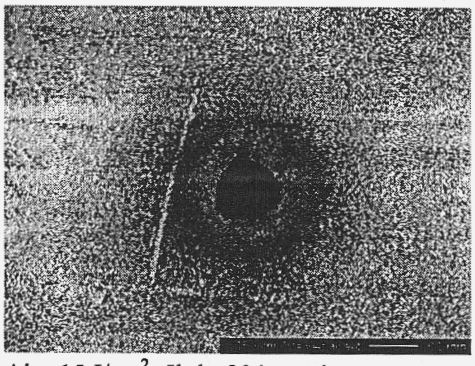

Air: 15 J/cm^2, 5brk=304 s, exit

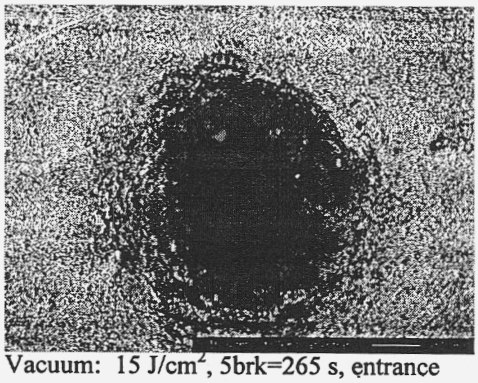

Vacuum: 15 J/cm^2, 5brk=265 s, entrance

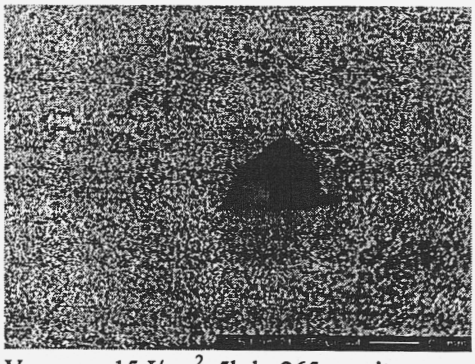

Vacuum: 15 J/cm^2, 5brk=265 s, exit

Figure 2.11p. Entrance and exit surfaces of holes drilled by 500-ps, 200-μm diameter laser spot on 0.9-mm thick 304 stainless steel at a fluence of 15 J/cm^2, showing the difference in shape and quality of holes drilled in vacuum and air.

2.5 Discussion

For shorter pulse-widths, the rate in vacuum is higher than that in air. There are a few possible explanations for this result. Short pulses tend to interact with air especially at higher fluences. This causes a degradation of beam quality at the part and therefore a lower drilling rate (compare the front-surface quality of any of the 15 J/cm^2 air/vacuum holes). There may also be a plasma/air interaction at the ablation site that could prevent the beam from efficiently ablating the fresh material. Oxidation may also play a role in the lower ablation rate in air. In a vacuum, there is no interaction with air of either the laser or the plasma, which leads to more efficient drilling and higher rates. There is also no chance of oxidation. At longer pulse widths, laser/air interaction is less causing the rates in air to be closer to those in vacuum.

As the drilling progresses, the rate slows down. This can also be explained in a number of ways. Once a hole is established, the laser energy may reflect off the walls of the hole, getting dispersed and not used for ablation. Because the walls of the holes may not be smooth, some of the laser energy may be absorbed into the walls. This is most apparent at longer pulse-widths and at higher fluences where the decrease in rate with depth is much more dramatic. Shorter pulses win out for deeper holes since they heat the plasma (ablated material) hotter which gives it a better chance of finding its way out of the hole.

3. Martensitic steel drilling

3.1 Introduction

An investigation was made to determine whether femtosecond pulses produce any significant effect on the microstructure of the surrounding material when laser drilling steel of interest for fuel injector components. Two 10-mil thick samples were provided by Oak Ridge National Laboratory (D. Ray Johnson). The samples were laser drilled at Lawrence Livermore National Laboratory and returned to Oak Ridge for analysis. A wide range of pulse duration (500 fs – 25 ps) and fluence (2-15 J/cm^2) was covered to try to determine where collateral effects might appear.

3.2 Samples (Phil Maziasz, ORNL)

10-mil thick 9Cr-1MoVNb martensitic steel foils:
Heat treatment 1 (Material #1) – normalized but not tempered. This is a non-standard fully-martensitic structure that is as hard as the material can be. Heating for any length of time beyond several seconds at 400-700 °C should soften the material (hardness profile would show this) and/or produce precipitation visible in the microstructure as evidence of heating during or after machining. Heating beyond 700 °C will produce coarser carbide precipitates and temper the martensite. Heating much above 800-900 °C will produce austenite that will transform back to martensite, if cooling is fast enough. Discoloration due to oxides will also produce visible measure of heating.

Heat treatment 2 (Material #2) – normalized and tempered. This is the standard microstructural and properties condition for this material in a wide range of engineering applications. This will not be very sensitive to heating below the temperating temperature of 760 °C, but will give a better measure of temperature exposure in the range of 800-900 °C due to carbide coarsening in the as-tempered structure. Exposure at temperatures above the austenite-start temperature (about 900 °C) will then become martensitic upon rapid cooling. Surface of foil should be cleaned so that oxide heat-tint will be evidence of lower temperatures.

3.3 Laser drilling

We used an 810-nm, nominally flat-top spatial mode, produced by overfilling a 5-mm round aperture and imaging the aperture with 25x demagnification. This resulted in a 200 μm diameter beam with peak fluence in the range of 2-15 J/cm^2. Since the imaging geometry resulted in the beam going through focus before the part, all drilling was done in vacuum to avoid air breakdown. A thin glass debris shield was used to shield the 10-cm focal length lens from the debris. The pulse duration was varied from 500 fs to 25 ps to ascertain whether there is any increase in thermal damage over this pulse duration range. This is important for system design, as the laser architecture changes dramatically

over this range (from Ti:sapphire, to Yb:YAG, to Nd:YAG, the latter two being directly diode-pumpable). The matrices of holes for the two samples and front and rear surface pictures of the drilled holes are tabulated below (see Table 3.1, Figs. 3.1a-c for results from material #1, and Table 3.2, Figs. 3.2a-c for results from material #2).

MATERIAL # 1

Row #	Hole #	Fluence	Rep Rate	Pulse With	Time
1	1	15 J/cm^2	100 Hz	500 fs	90s
	2	15 J/cm^2	100 Hz	500 fs	225s
	3	15 J/cm^2	100 Hz	1 ps	90s
	4	15 J/cm^2	100 Hz	1 ps	225s
	5	15 J/cm^2	100 Hz	5 ps	90s
2	1	15 J/cm^2	100 Hz	5 ps	225s
	2	15 J/cm^2	100 Hz	25 ps	90s
	3	15 J/cm^2	100 Hz	25 ps	225s
	4	5 J/cm^2	100 Hz	500 fs	180s
	5	5 J/cm^2	100 Hz	500 fs	450s
3	1	5 J/cm^2	100 Hz	1 ps	180s
	2	5 J/cm^2	100 Hz	1 ps	450s
	3	5 J/cm^2	100 Hz	5 ps	180s
	4	5 J/cm^2	100 Hz	5 ps	450s
	5	5 J/cm^2	100 Hz	25 ps	180s
4	1	5 J/cm^2	100 Hz	25 ps	450s
	2	2 J/cm^2	100 Hz	500 fs	300s
	3	2 J/cm^2	100 Hz	500 fs	1500s
	4	2 J/cm^2	100 Hz	1 ps	300s
	5	2 J/cm^2	100 Hz	1 ps	1500s
5	1	2 J/cm^2	100 Hz	5 ps	300s
	2	2 J/cm^2	100 Hz	5 ps	1500s

Table 3.1. Matrix of holes drilled in vacuum in Material #1 (non-tempered) by short laser pulses (500 fs – 25 ps), at different fluences, and for different times.

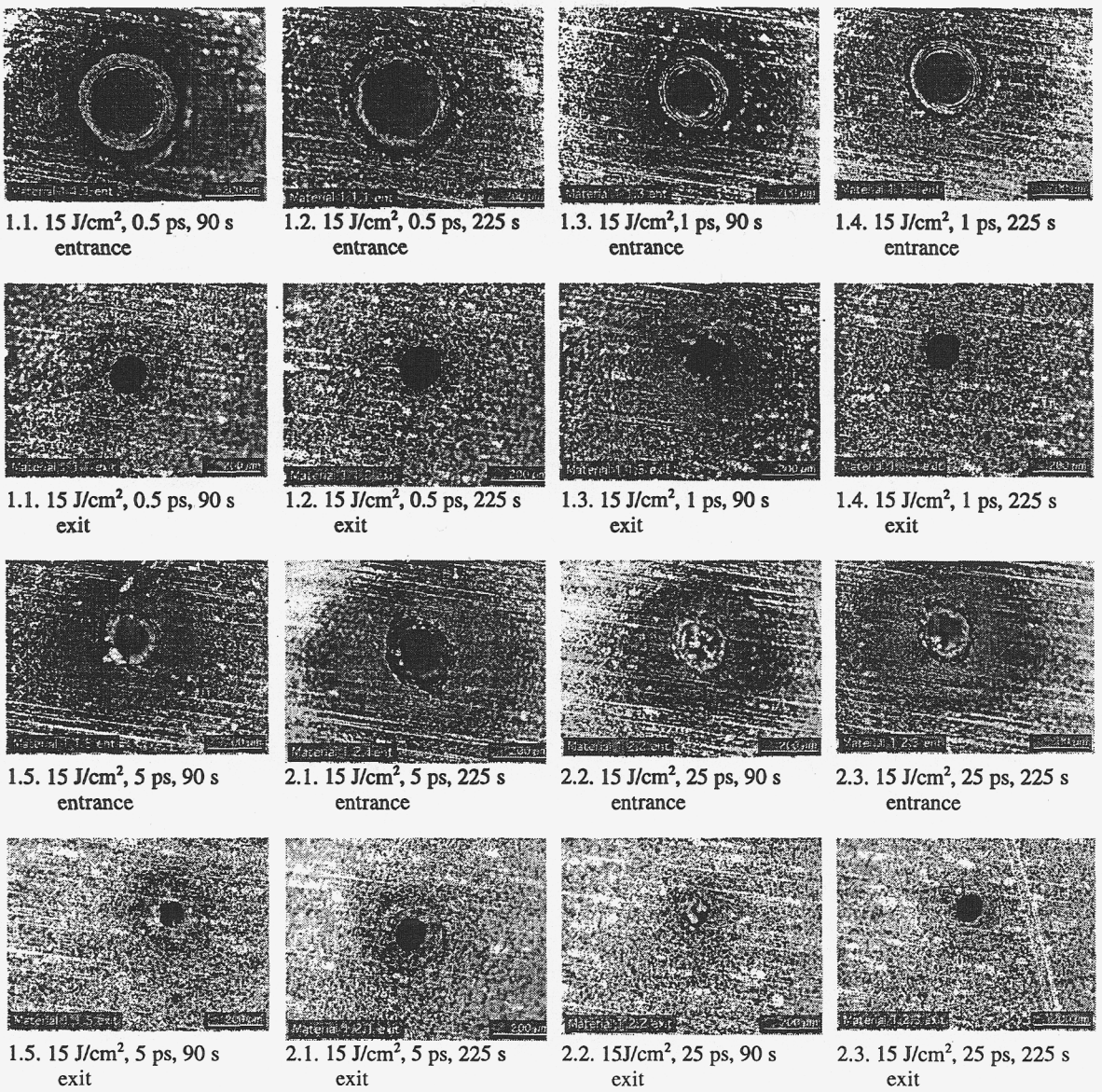

1.1. 15 J/cm², 0.5 ps, 90 s entrance | 1.2. 15 J/cm², 0.5 ps, 225 s entrance | 1.3. 15 J/cm²,1 ps, 90 s entrance | 1.4. 15 J/cm², 1 ps, 225 s entrance

1.1. 15 J/cm², 0.5 ps, 90 s exit | 1.2. 15 J/cm², 0.5 ps, 225 s exit | 1.3. 15 J/cm², 1 ps, 90 s exit | 1.4. 15 J/cm², 1 ps, 225 s exit

1.5. 15 J/cm², 5 ps, 90 s entrance | 2.1. 15 J/cm², 5 ps, 225 s entrance | 2.2. 15 J/cm², 25 ps, 90 s entrance | 2.3. 15 J/cm², 25 ps, 225 s entrance

1.5. 15 J/cm², 5 ps, 90 s exit | 2.1. 15 J/cm², 5 ps, 225 s exit | 2.2. 15J/cm², 25 ps, 90 s exit | 2.3. 15 J/cm², 25 ps, 225 s exit

Figure 3.1a. Front and rear surface pictures of the holes drilled in Material #1 (non-tempered) at 15 J/cm², various pulse durations, and at 100 Hz for the times indicated. Note the quality of the holes degrades as the pulse duration increases to > 1 ps.

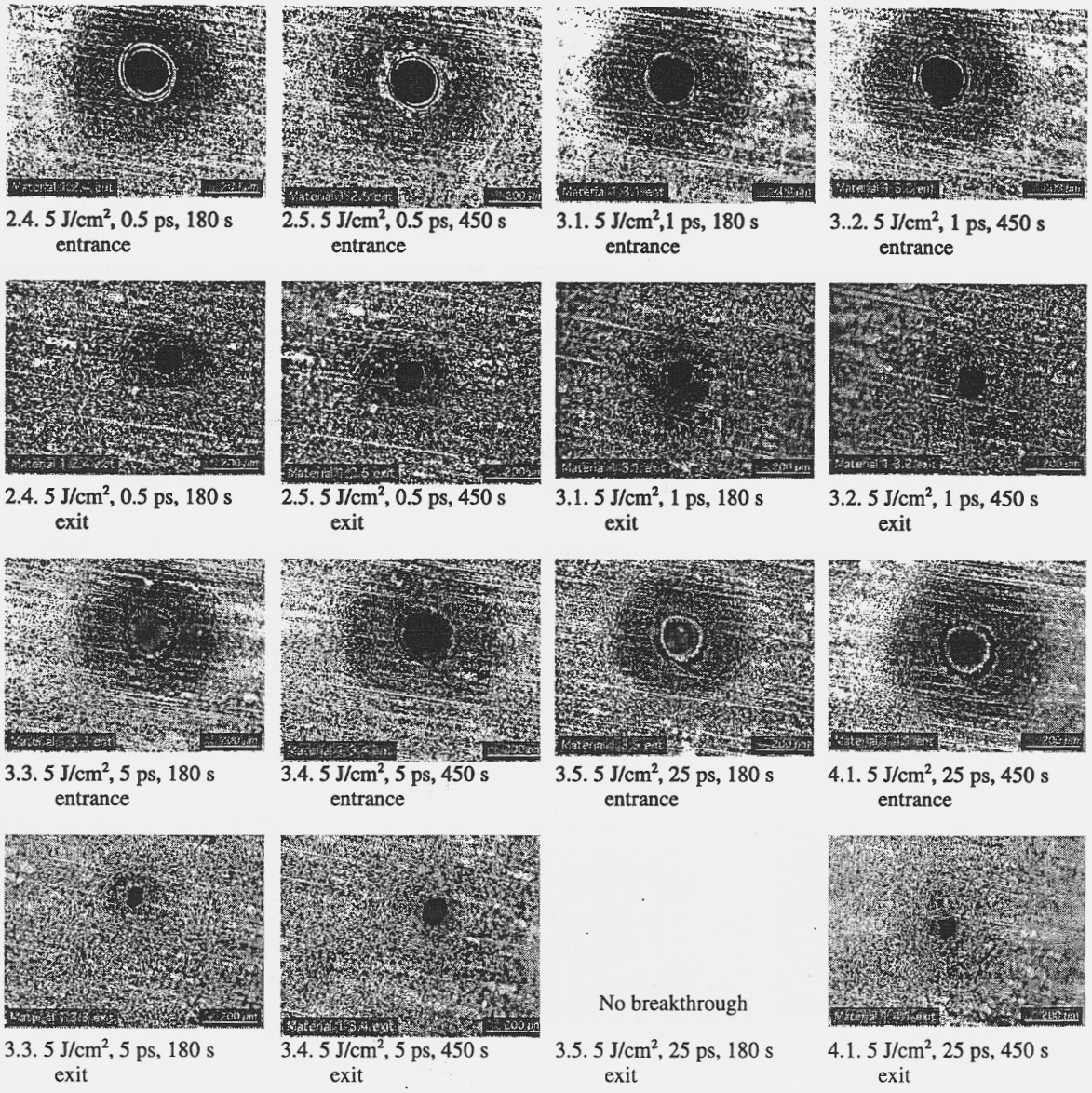

Figure 3.1b. Front and rear surface pictures of the holes drilled in Material #1 (non-tempered) at 5 J/cm², various pulse durations, and at 100 Hz for the times indicated. Holes of good quality were observed at pulse durations < 5 ps.

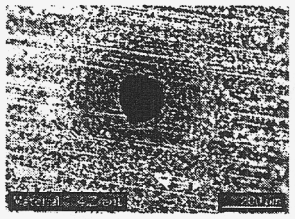

4.2. 2 J/cm^2, 0.5 ps, 300 s entrance

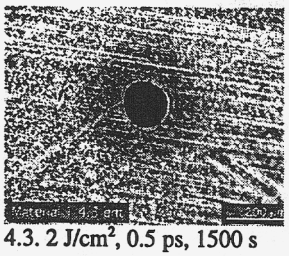

4.3. 2 J/cm^2, 0.5 ps, 1500 s entrance

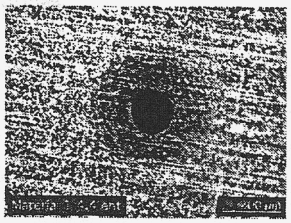

4.4. 2 J/cm^2,1 ps, 300 s entrance

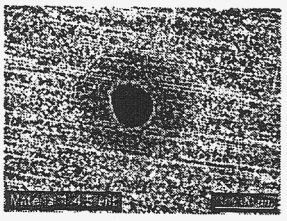

4.5. 2 J/cm^2, 1 ps, 1500 s entrance

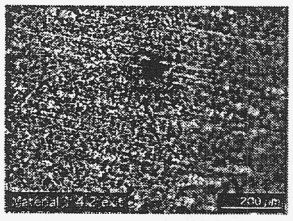

4.2. 2 J/cm^2, 0.5 ps, 300 s exit

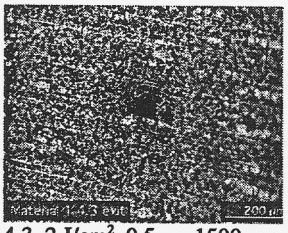

4.3. 2 J/cm^2, 0.5 ps, 1500 s exit

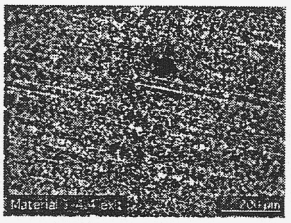

4.4. 2 J/cm^2, 1 ps, 300 s exit

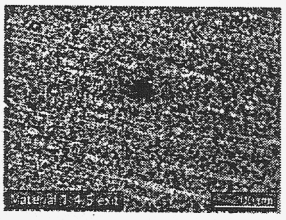

4.5. 2 J/cm^2, 1 ps, 1500 s exit

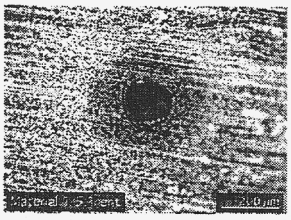

5.1. 2 J/cm^2, 5 ps, 300 s entrance

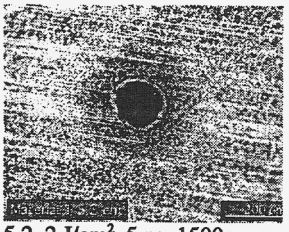

5.2. 2 J/cm^2, 5 ps, 1500 s entrance

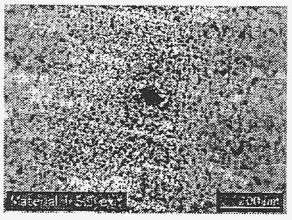

5.1. 2 J/cm^2, 5 ps, 300 s exit

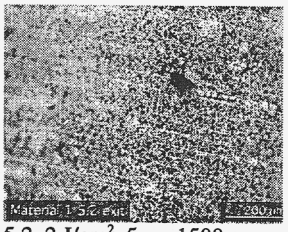

5.2. 2 J/cm^2, 5 ps, 1500 s exit

Figure 3.1c. Front and rear surface pictures of the holes drilled in Material #1 (non-tempered) at 2 J/cm^2, various pulse durations, and at 100 Hz for the times indicated. Holes of good quality were observed at pulse durations < 5 ps.

MATERIAL #2

Row #	Hole #	Fluence	Rep Rate	Pulse With	Time
1	1	15 J/cm^2	100 Hz	5 ps	90s
	2	15 J/cm^2	100 Hz	5 ps	225s
	3	15 J/cm^2	100 Hz	500 fs	90s
	4	15 J/cm^2	100 Hz	500 fs	225s
	5	15 J/cm^2	100 Hz	1 ps	90s
2	1	15 J/cm^2	100 Hz	1 ps	225s
	2	15 J/cm^2	100 Hz	25 ps	90s
	3	15 J/cm^2	100 Hz	25 ps	225s
	4	5 J/cm^2	100 Hz	500 fs	180s
	5	5 J/cm^2	100 Hz	500 fs	450s
3	1	5 J/cm^2	100 Hz	1 ps	180s
	2	5 J/cm^2	100 Hz	1 ps	450s
	3	5 J/cm^2	100 Hz	5 ps	180s
	4	5 J/cm^2	100 Hz	5 ps	450s
	5	5 J/cm^2	100 Hz	25 ps	180s
4	1	5 J/cm^2	100 Hz	25 ps	450s
	2	2 J/cm^2	100 Hz	500 fs	300s
	3	2 J/cm^2	100 Hz	500 fs	1500s
	4	2 J/cm^2	100 Hz	1 ps	300s
	5	2 J/cm^2	100 Hz	1 ps	1500s
5	1	2 J/cm^2	100 Hz	5 ps	300s
6	1	2 J/cm^2	100 Hz	5 ps	1500s

Table 3.2. Matrix of holes drilled in vacuum in Material #2 (tempered) by short laser pulses (500 fs – 25 ps), at different fluences, and for different times.

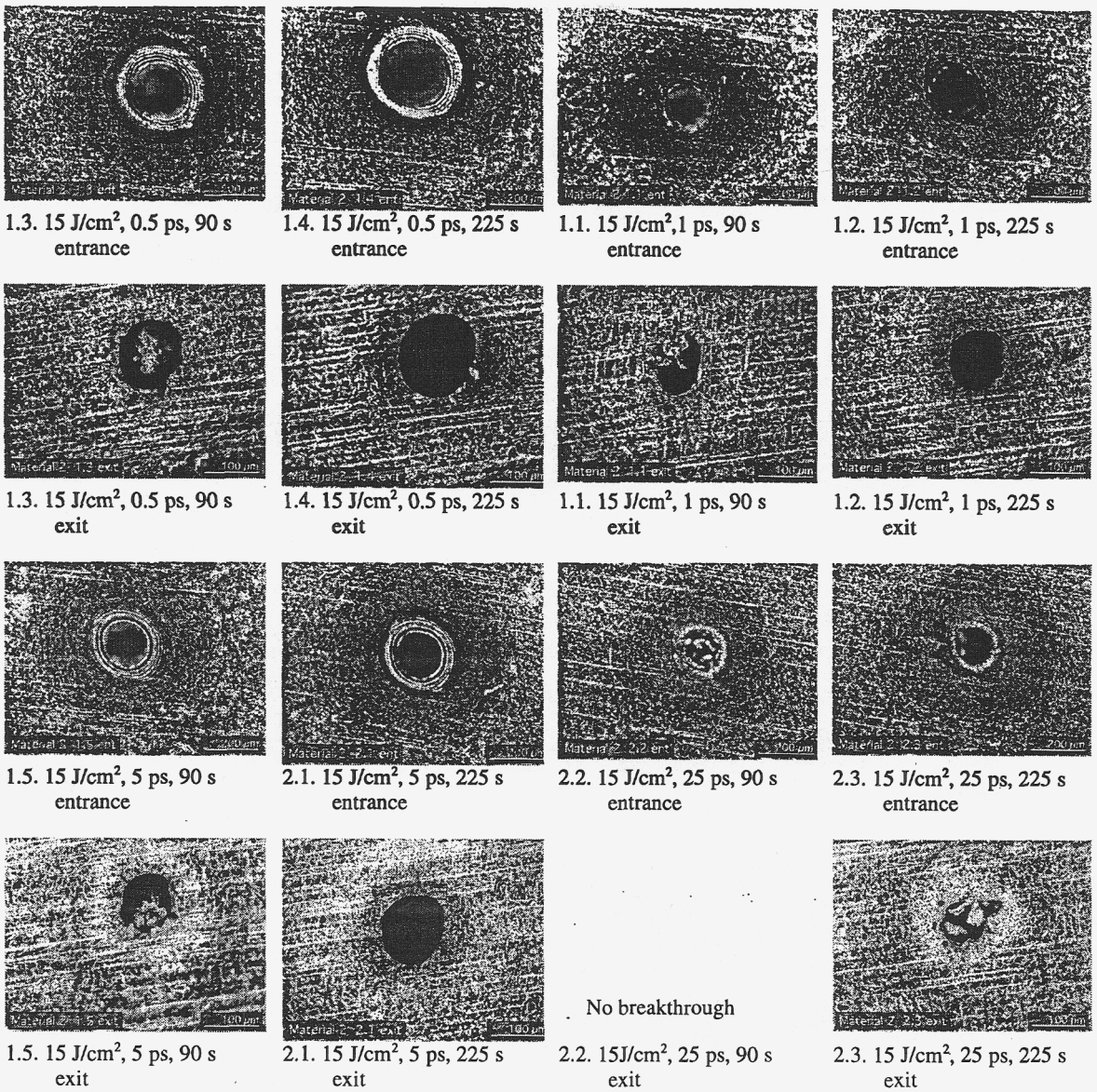

Figure 3.2a. Front and rear surface pictures of the holes drilled in Material #2 (tempered) at 15 J/cm², various pulse durations, and at 100 Hz for the times indicated. Note the quality of the holes degrades as the pulse duration increases to > 1 ps.

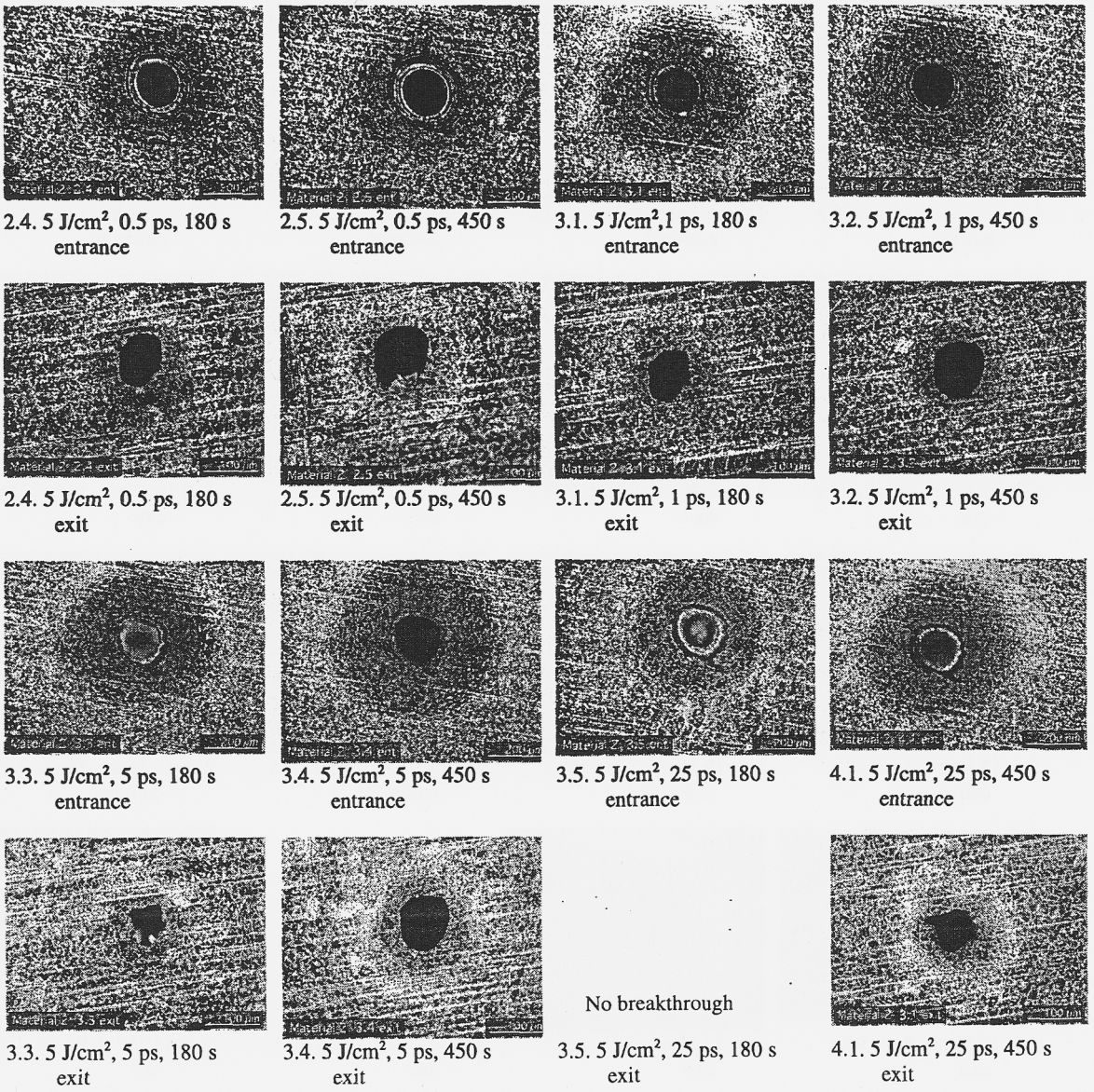

2.4. 5 J/cm^2, 0.5 ps, 180 s entrance | 2.5. 5 J/cm^2, 0.5 ps, 450 s entrance | 3.1. 5 J/cm^2,1 ps, 180 s entrance | 3.2. 5 J/cm^2, 1 ps, 450 s entrance

2.4. 5 J/cm^2, 0.5 ps, 180 s exit | 2.5. 5 J/cm^2, 0.5 ps, 450 s exit | 3.1. 5 J/cm^2, 1 ps, 180 s exit | 3.2. 5 J/cm^2, 1 ps, 450 s exit

3.3. 5 J/cm^2, 5 ps, 180 s entrance | 3.4. 5 J/cm^2, 5 ps, 450 s entrance | 3.5. 5 J/cm^2, 25 ps, 180 s entrance | 4.1. 5 J/cm^2, 25 ps, 450 s entrance

3.3. 5 J/cm^2, 5 ps, 180 s exit | 3.4. 5 J/cm^2, 5 ps, 450 s exit | No breakthrough 3.5. 5 J/cm^2, 25 ps, 180 s exit | 4.1. 5 J/cm^2, 25 ps, 450 s exit

Figure 3.2b. Front and rear surface pictures of the holes drilled in Material #2 (tempered) at 5 J/cm^2, various pulse durations, and at 100 Hz for the times indicated. Holes of good quality were observed at pulse durations < 5 ps.

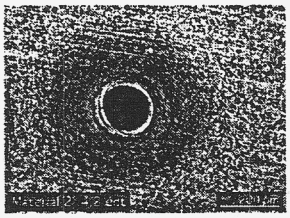

4.2. 2 J/cm^2, 0.5 ps, 300 s entrance

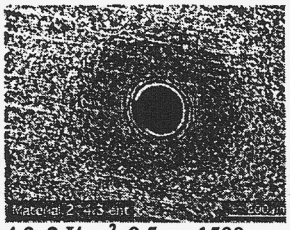

4.3. 2 J/cm^2, 0.5 ps, 1500 s entrance

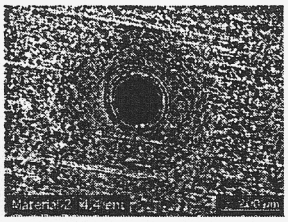

4.4. 2 J/cm^2,1 ps, 300 s entrance

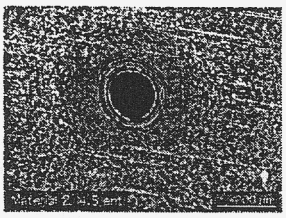

4.5. 2 J/cm^2, 1 ps, 1500 s entrance

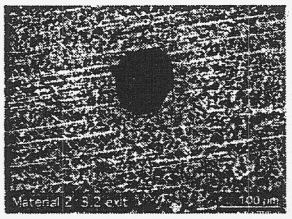

4.2. 2 J/cm^2, 0.5 ps, 300 s exit

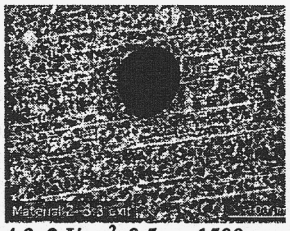

4.3. 2 J/cm^2, 0.5 ps, 1500 s exit

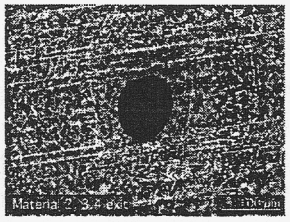

4.4. 2 J/cm^2, 1 ps, 300 s exit

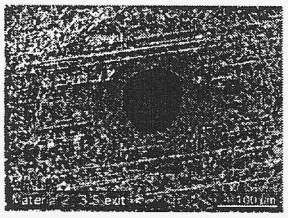

4.5. 2 J/cm^2, 1 ps, 1500 s exit

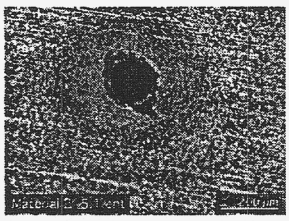

5.1. 2 J/cm^2, 5 ps, 300 s entrance

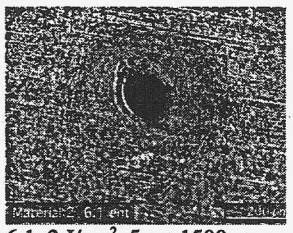

6.1. 2 J/cm^2, 5 ps, 1500 s entrance

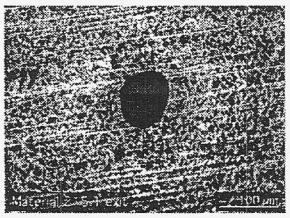

5.1. 2 J/cm^2, 5 ps, 300 s exit

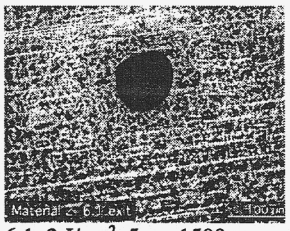

6.1. 2 J/cm^2, 5 ps, 1500 s exit

Figure 3.2c. Front and rear surface pictures of the holes drilled in Material #2 (tempered) at 2 J/cm^2, various pulse durations, and at 100 Hz for the times indicated. Holes of good quality were observed at pulse durations < 5 ps.

3.4 ORNL Analysis

PRELIMINARY EVALUATION OF FEMTOSECOND LASER FOR HOLE-DRILLING IN DIESEL FUEL-INJECTORS

Philip J. Maziasz, D. Ray Johnson (ORNL)

Introduction

The Office of Heavy Vehicle Technologies Propulsion Materials Program has a significant interest in diesel engine fuel injectors. Fuel injection and air handling make up approximately 50% of the complexity and cost of heavy-duty diesel engines. In order to meet future exhaust emissions and fuel efficiency regulations and targets, it will be necessary to improve the precision and performance of diesel fuel injectors.

One particular concern is the precision and cost of the holes in the fuel injector tip. The size and shape of these holes in very important to the resulting spray pattern from the injector, which, in turn, affects the efficiency of combustion and resulting exhaust emissions. The injector tips are made of high-strength steel. The holes are drilled by means of conventional wire EDM technology.

The femtosecond laser is being investigated as a potentially improved method for drilling the holes in the fuel injector tip. The very short pulse length of the femtosecond laser allows, in theory, the removal of material one atom at a time by ionizing each atom and then stripping it away from the surface of the workpiece without passing thermal energy from the focused laser beam along to the surrounding metal atoms.

A simple experiment was designed to determine whether or not a heat effected zone surrounded holes drilled in steel foil by the femtosecond laser. LLNL drilled holes in specimens of a heat-resistant martensitic 9Cr-1MoVNb steel foils (supplied in two metallurgical conditions by ORNL) using a range of parameters with the femtosecond laser. ORNL then performed post-laser-drilling analysis with additional metallographic examination of the material surrounding the holes. This short report summarizes the metallographic analysis; the details of actual laser parameters and individual photographs of each hole (front and back sides of foil) were reported by Brent Stuart (LLNL) and are included as an attachment to this report.

Results and Conclusions

The 9Cr-1MoVNb steel foils (10 mils or 0.254 mm thick) were used as a hole-drilling test substrate because they had somewhat similar physical and mechanical properties to the high-strength steels used in the actual fuel-injector nozzles, and they were conveniently available as foil. We used the steel in the untempered (fully-martensitic) as well as the tempered-martensitic (1h at 760°C) conditions, so that the material would give some sort of microstructural evidence of maximum temperature exposure for each

material (carbide precipitation for untempered material occurs in the 500-760°C range and carbide-coarsening for the tempered material occurs much above 760-800°C). It should also be kept in mind that the thinner foil material is also an easier hole-drilling test than the actual thicker component, and that the 9Cr steel is much more heat- and oxidation-resistant than the typical fuel-injector steel.

Figure 3.3 shows an actual fuel-injector nozzle with fine EDM-drilled holes (illuminated by backlighting), while Figs. 3.4a and 3.4b show the arrays of holes drilled with the different laser conditions in both test foils. The conditions are listed for each hole in tables in the attached LLNL report (Tables 3.1 and 3.2), with material #2 being tempered and material #1 being untempered 9Cr-1MoVNb steel. The indexing reference is 1.1, with the first digit being the row index and the second digit being the column index.

Only two laser-drilled holes did not penetrate, and the top two rows with the highest laser power settings show the largest craters on the front side of the holes. All of the holes appear to be conical, although the ratio of inlet size to exit size is larger for the holes drilled at the higher fluence. While the large colored circle around the general array of holes may be due to vaporized material redepositing, the smaller circles around each hole appear to be thin, transparent oxides from heating, which suggests that the material immediately adjacent to each hole is exposed to at least 450-550°C during laser-drilling. Metallography of the better holes (2.4 in Fig. 3.4a and 3.2 in Fig. 3.4b) on each foil shows no gross changes in microstructure in either material (Fig. 3.6). However, higher magnification examination of the untempered material (Fig. 3.7) does show what appears to be some tempering and carbide precipitation in a 5-15 μm region adjacent to the holes, which would suggest temperatures as high as 650-700°C were reached, consistent with the oxide halo. Similar examination of the tempered martensitic structures shows no evidence at these magnifications of overtempering, suggesting that temperatures did not exceed 700-750°C.

These preliminary results indicate that the femtosecond laser holes suffer collateral damage in the form of cone-shaped material removal as well as significant heat deposition in the material immediately adjacent to the holes. Such results may get worse on thicker target material, and the heating effects on a low-alloy or less heat-resistant material would certainly soften it or adversely affect hardness and wear. How this lab-based laser technology relates to commercial laser-drilling technology remains to be established. Certainly the claims of a gentle process that removes atoms one or a few at a time is not substantiated by these preliminary results, and more work (e.g., other fluences, times, frequencies, etc.) would be needed to prove the feasibility of this technique as an alternate hole-drilling technology.

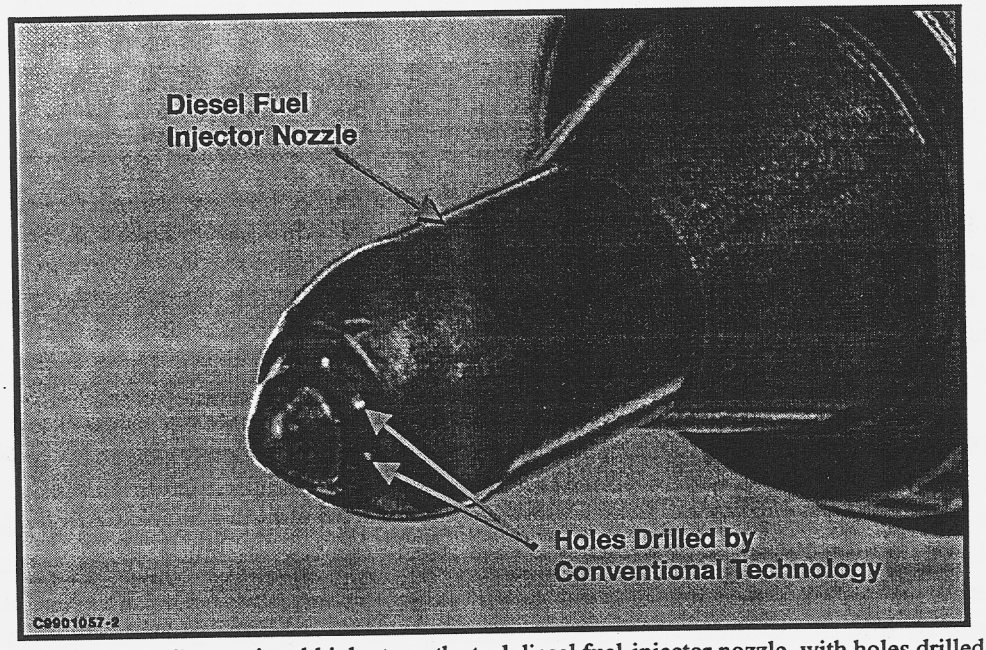

Figure 3.3. Conventional high-strength steel diesel fuel-injector nozzle, with holes drilled by conventional wire-EDM methods.

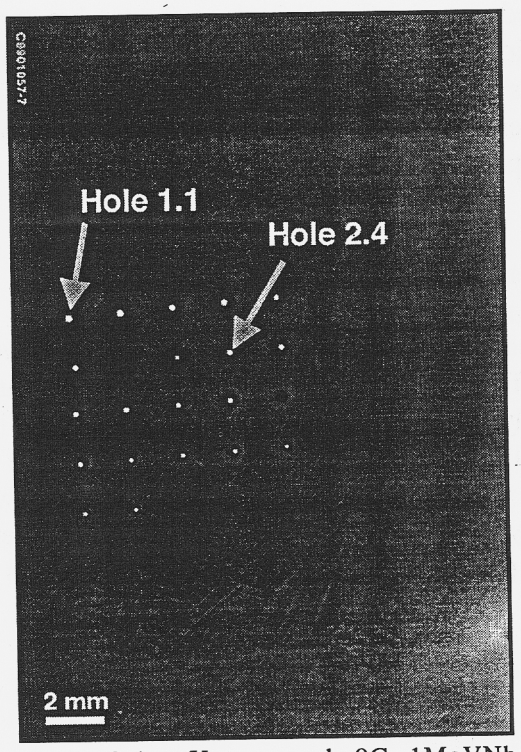

Figure 3.4a. Untempered 9Cr-1MoVNb martensitic steel foil with array of holes drilled by short-pulse laser. Hole 1.1 drilled at 15 J/cm^2, 500 fs, 90s. Hole 2.4 drilled at 5 J/cm^2, 500 fs, 180 s.

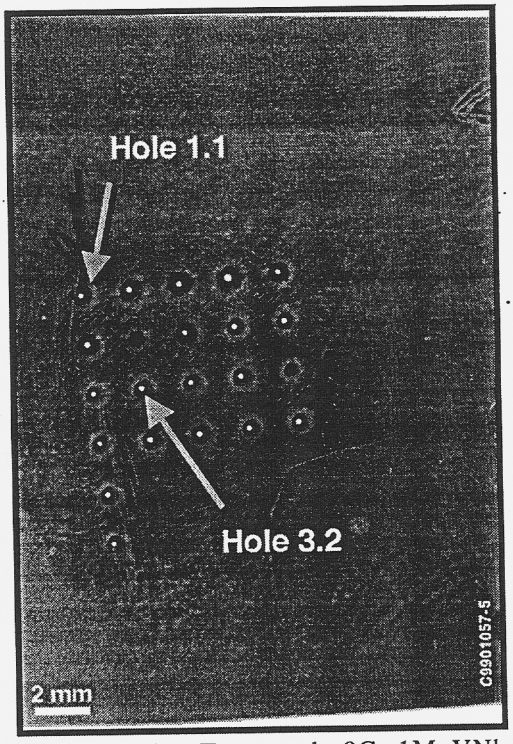

Figure 3.4b. Tempered 9Cr-1MoVNb martensitic steel foil with array of holes drilled by short-pulse laser. Hole 1.1 drilled at 15 J/cm^2, 5 ps, 90s. Hole 3.2 drilled at 5 J/cm^2, 1 ps, 450 s.

Fig. 3.5. Computed X-ray Tomography Image showing cross-section of holes 1.2 - 1.5 in Material 2. The holes are conical; the diameter of the inlet hole is approximately twice that of the outlet hole.

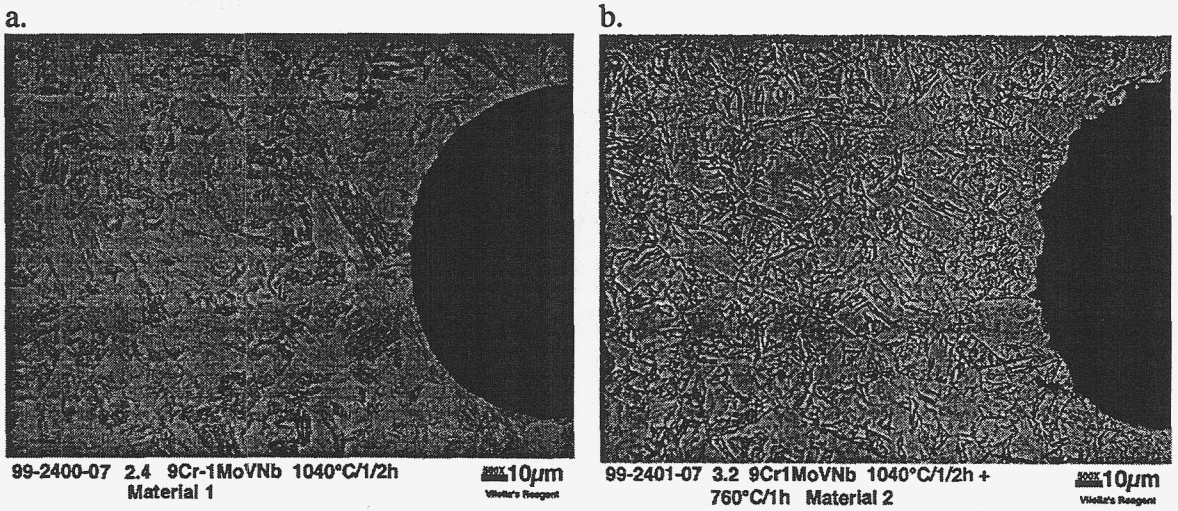

Fig. 3.6. Lower magnification metallography of the microstructure adjacent to individual holes (also identified in Fig. 3.4 for a) untempered and b)tempered 9Cr-1MoVNb martensitic steel.

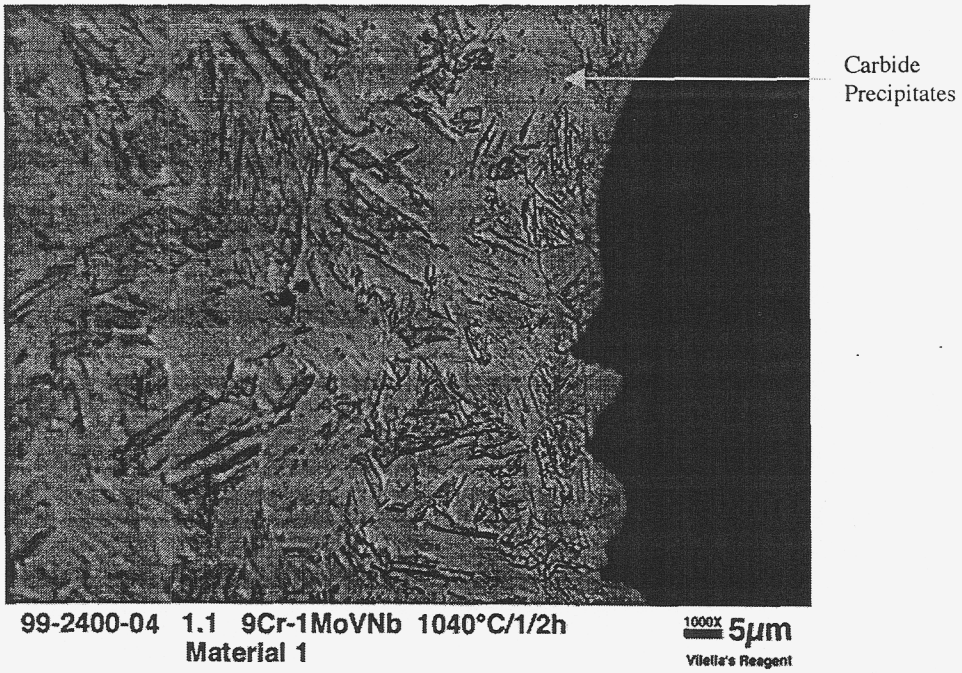

Fig. 3.7. Higher magnification metallography showing tempering effects and carbide precipitation very near the hole (1.1, identified in Fig. 3.4a in the untempered 9Cr-1MoVNb martensitic steel.

3.5 LLNL Conclusions

The lower fluence holes (Hole 2.4 (#1) at 5 J/cm^2, 500 fs and hole 3.2 (#2) at 5 J/cm^2, 1 ps) that were analyzed by ORNL showed little evidence of microstructural change. The higher fluence hole (Hole 1.1 (#1) at 15 J/cm^2, 500 fs) showed some evidence of tempering and carbide precipitation according to ORNL. We know from drilling experience that 15 J/cm^2 is fairly high for the surface of metals and often results in lower quality holes, especially through the thinner materials. We also see evidence of the carbide precipitates throughout Figure 3.7 and not just in the 5-15 micron region near the edge of the hole. We suggest also that the indication of an oxide layer be tested by x-ray fluorescence analysis. It is difficult to reach general conclusions based on the analysis of three holes in thin material. A complete analysis of all the holes and a continued investigation into deeper holes would be very useful. This could also be accompanied by a direct comparison to holes drilled with a conventional long-pulse (10-200 ns) green or IR laser.

4. Drilling of Ceramics and Metal-Matrix Composites

4.1 Alumina

We drilled a set of holes in alumina to determine hole quality and drill rates. We used 405 nm pulses at 100 Hz to drill 200-micron diameter holes. The pulse energy was 1.1 mJ (3.5 J/cm^2) and the pulse-width was 1 ps. A 5-mm diameter iris was imaged by a 10-cm focal length lens to achieve a flat-top profile beam with a 200 micron diameter. A half wave plate was spun in the beam to create circular polarization. The samples were 1 mm thick.

Holes were drilled for various times (Table 4.1) to determine rates and hole quality. It was observed that a bright plasma was emitted from the ceramic for the first one or two seconds, and then the ceramic would begin to glow around the area of the beam.

SEM photos were taken of the holes after coating the ceramic for optimized contrast. The drilling times (Fig. 4.1) and photos (Fig. 4.2) are presented below. It appears that the drilling stalled out after 30 sec, as there was no evidence of breakthrough. This is not surprising given the relatively low fluence.

Hole #	Energy (mJ)	Time	Depth (micron)	Pulse width	Rate (micron/s)
101	1.1	5 min		1 ps	
102	1.1	10 min		1 ps	
103	1.1	2 min		1 ps	
201	1.1	1 min		1 ps	
202	1.1	30 s		1 ps	
203	1.1	10 s	300	1 ps	30
301	1.1	1 s	29	1 ps	29
302	1.1	3 s	75	1 ps	25
303	1.1	5 s	133	1 ps	26.6
				Average rate = 27.7	

Table 4.1. Matrix of holes on alumina drilled by 1-ps, 1.1 mJ laser pulses at 100 Hz.

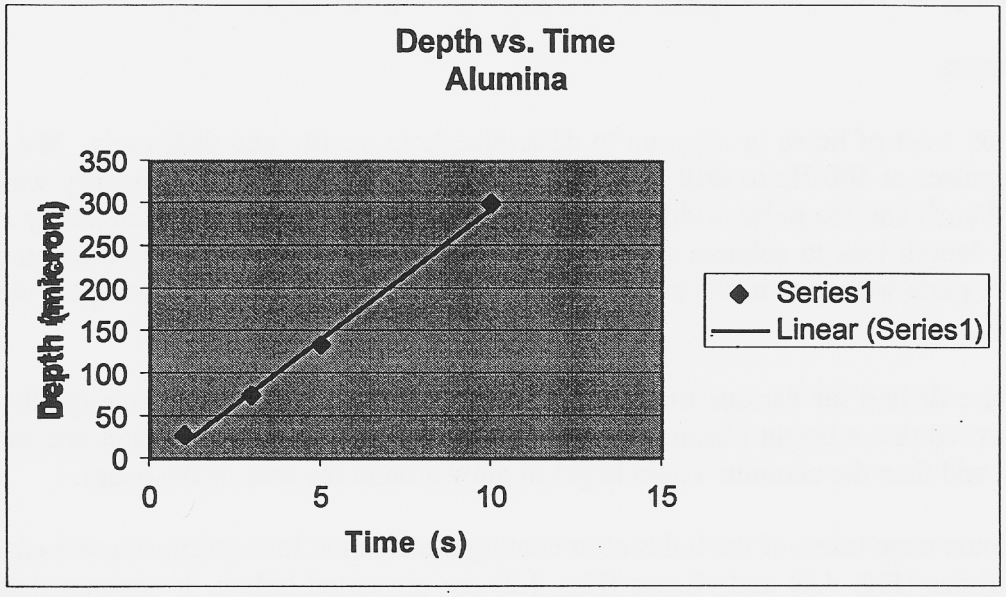

Figure 4.1. Depth of holes drilled in alumina by 1-ps, 1.1 mJ pulses at 100 Hz.

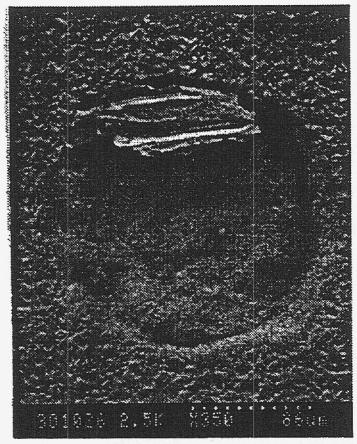

#301 1 second

#302 3 seconds

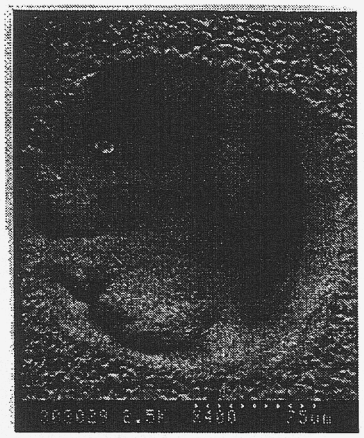

#303 5 seconds

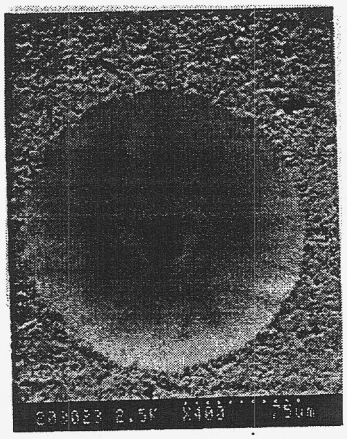

#203 10 seconds

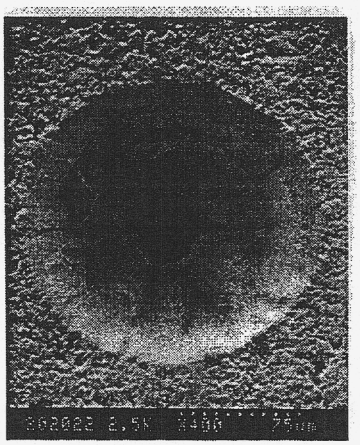

#202 30 seconds

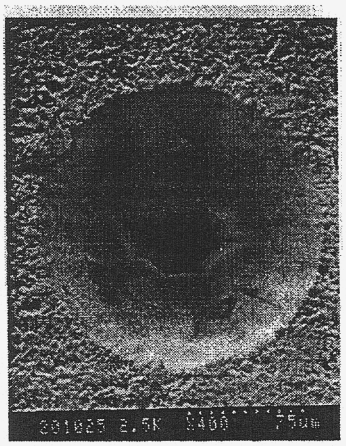

#201 1 minute

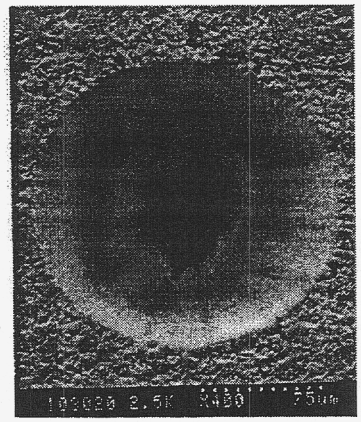

#103 2 minutes

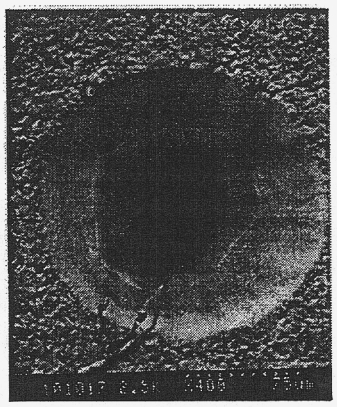

#101 5 minutes

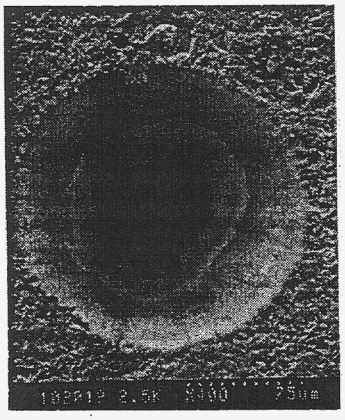

#102 10 minutes

Figure 4.2. Front surface of holes drilled in alumina by 1-ps, 1.1 mJ, 405 nm pulses at 100 Hz.

4.2 Zirconia

We attempted to laser-drill a large diameter hole (900 μm) through a relatively thick (9 mm) piece of zirconia. This is a configuration of interest in ceramic fuel-injector components. The first test was to determine whether we could even drill a small hole all the way through the 9 mm (this was much thicker than anything else we typically drill). We knew it would take a high fluence, so we focused the beam down to 130 μm, which gave a fluence of 70 J/cm^2 at an energy per pulse of 4.6 mJ. Under these conditions, we were able to drill a small hole all the way through the zirconia (Figure 4.3).

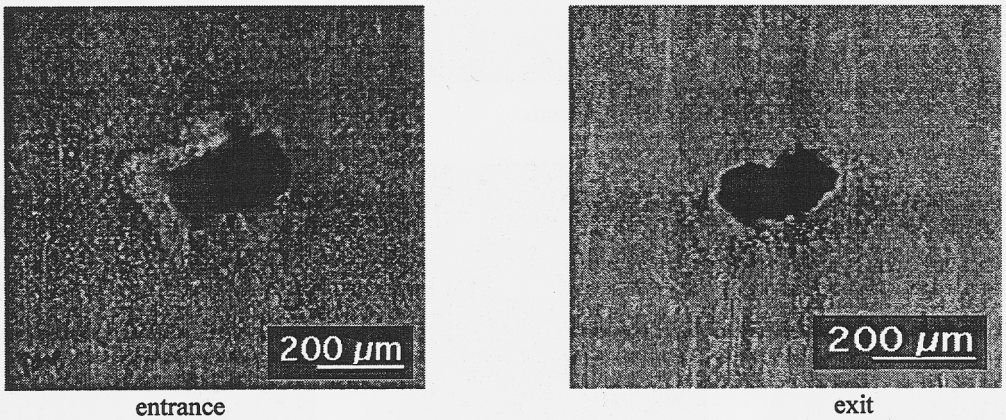

entrance exit

Figure 4.3 Hole drilled through 9 mm of zirconia at 70 J/cm^2.

Next, we rotated a 100-μm diameter laser spot about a radius of 900 μm in an attempt to "core drill" through the 9-mm zirconia. Figure 4.4 shows the entrance surface and cross section of the resulting hole. The ablation stalled out after approximately 4-mm depth due to losses of laser energy in reaching the bottom of the long, narrow slot, and due to the difficulty in the debris finding its way out of the hole. This would be much more successful by removing the central core, allowing easy laser access and a clear path for the ejected material. The penalty is a much greater volume of material must be removed.

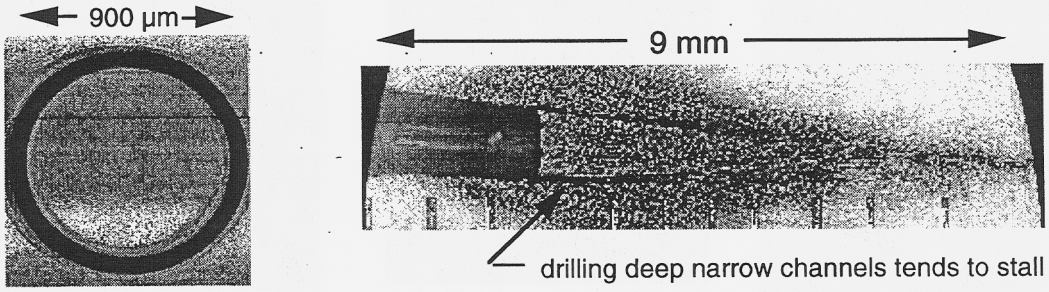

Figure 4.4 Top view and cross section of hole "core-drilled" in zirconia.

Even though the "core-drill" did not go completely through, the initial 3 mm resulted in a very high quality hole with no evidence of microcracking (Figure 4.5).

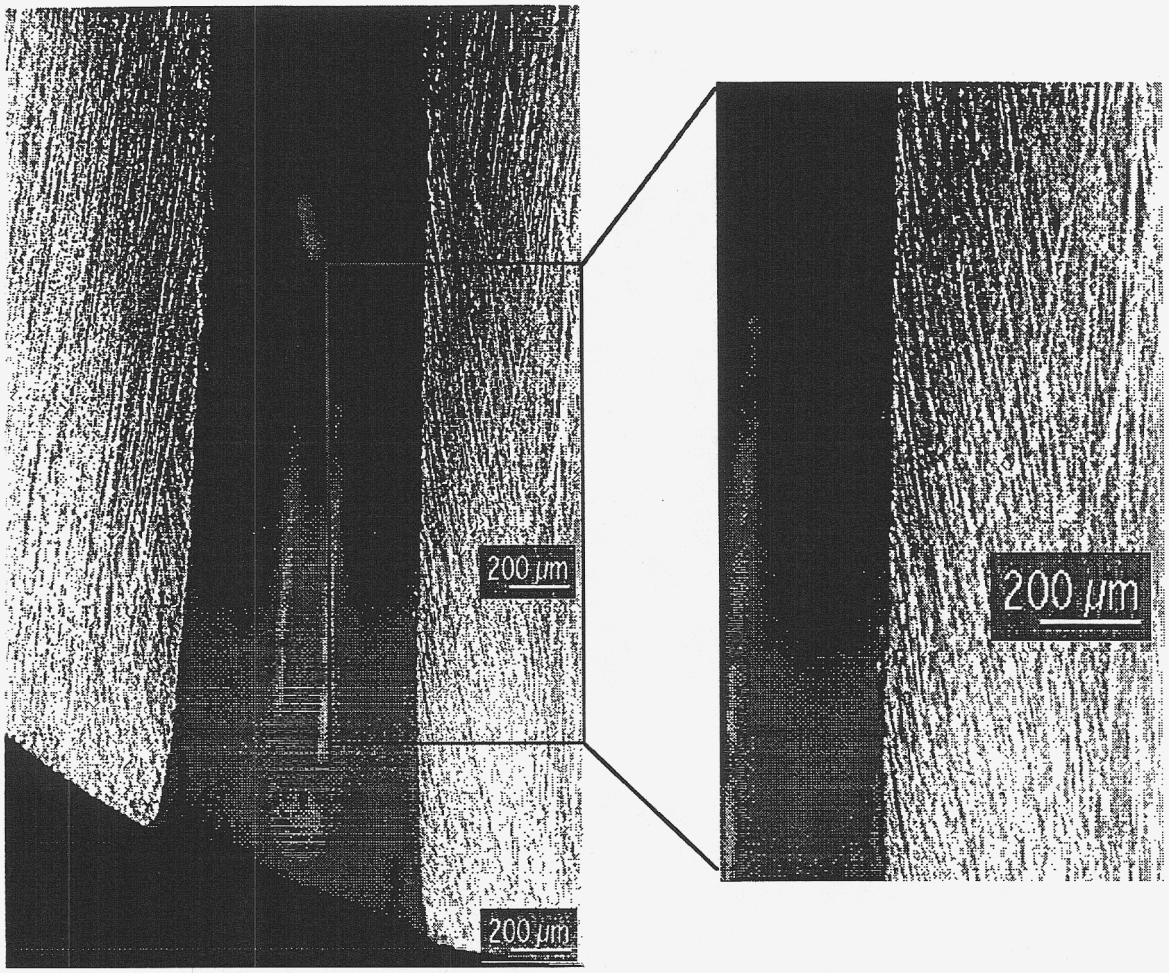

Figure 4.5 Cross section of initial 3 mm "core-drilled" in zirconia shows no evidence of microcracking.

4.3 Metal-Matrix Composite

We made an initial attempt at cutting a metal-matrix composite with our femtosecond laser system. The sample was a 2-mm thick silicon carbide reinforced aluminum composite. We used 150-fs, 1.3-mJ pulses focused to 150 μm to cut a 1-mm long slot in the composite (see Fig. 4.6). The relatively low fluence of 15 J/cm^2 precluded complete clean-out on the back side, but the quality of the cut from the front surface was excellent. A close-up of the entrance side of a different cut (where the energy was ramped slowly to 1 mJ) is shown in Figure 4.7.

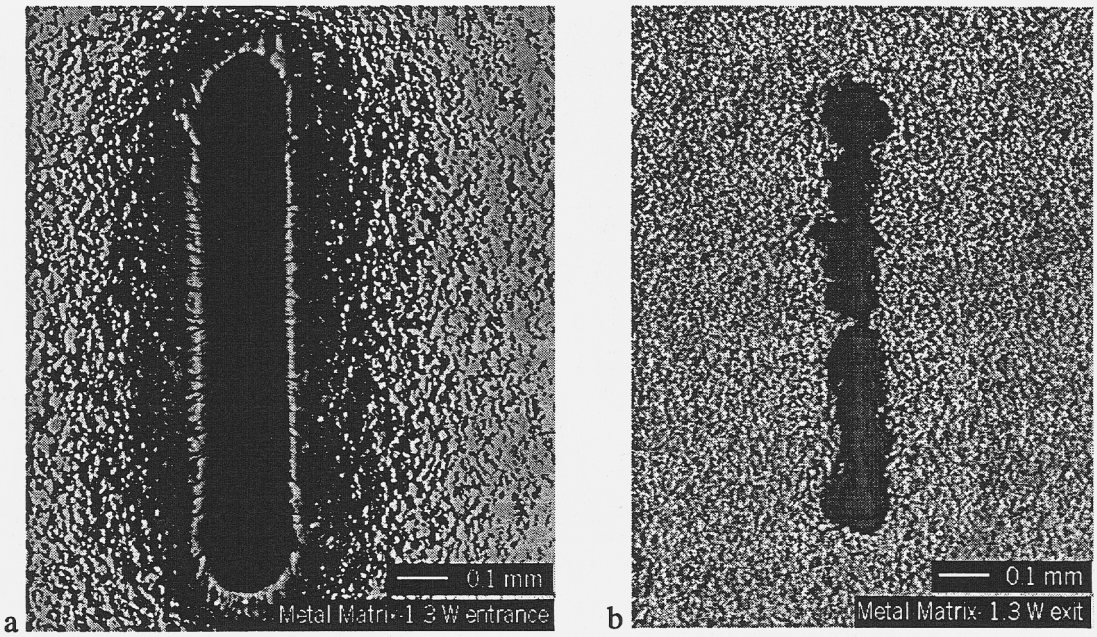

Figure 4.6. (a) entrance, and (b) exit surfaces of cut at 15 J/cm^2 in silicon carbide reinforced aluminum composite.

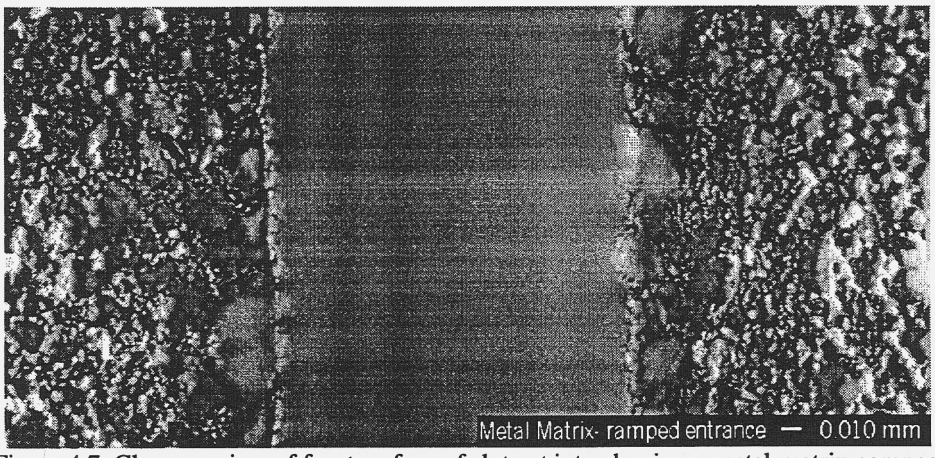

Figure 4.7. Close-up view of front surface of slot cut into aluminum metal-matrix composite. Energy was ramped to 1.3 mJ (15 J/cm^2).

4.4 Conclusions

Drilling of ceramics requires relatively high fluence to go through 1-mm thickness or more. The low-fluence drilling of alumina showed considerable taper and eventual stall-out. Beam motion with a high-fluence spot will likely help in being able to drill with straighter walls and flatter bottoms. We also see evidence of the same channel formation that appears in drilling metals. Optimization of the drilling conditions for this class of materials is necessary and should lead to a new processing tool for these difficult-to-machine materials.

5 Summary and future directions

5.1 Summary

During the initial phase of this research work, we focused on three technical areas that have immediate application to the transportation industry. A brief summary of our test results is described here:

1) Comparison of ultrashort-pulse drilling in air and vacuum for various pulse-durations: (0.15, 1, 20, 500 ps, the materials are stainless steel and aluminum)

Drilling of blind-holes:

- At constant fluence, the material removal rate decreases as the depth of the hole increases. The decrease in rate with increased depth is more apparent for drilling with long pulses. There is no appreciable difference of the slopes (rate-change) between holes drilled in air and holes drilled in vacuum.

- For short pulse-durations (0.15 ps and 1 ps), the drilling rate in vacuum was higher than in air. The difference was greater for aluminum and smaller for stainless steel.

- For long pulse-durations (20 ps and 500 ps), the rates were similar in air and vacuum.

- At constant fluence, the material removal rate decreases with increasing pulse-duration.

Drilling of through-holes:

- The breakthrough times were generally shorter in vacuum than air.

- The time required for achieving breakthrough in aluminum and stainless steel increases with pulse-duration.

- At low fluence level (3 J/cm^2), breakthrough in aluminum can only be achieved using 0.15 ps pulses.

- The breakthrough times for stainless steel are generally shorter than that for aluminum.

- Holes produced in vacuum generally have better shape and quality.

Our drilling data obtained from *air* and *vacuum* clearly indicated that laser-air interaction and oxidation of the metal surfaces under laser irradiation have played an important role in the drilling process. In general, hole-drillings in stainless and aluminum are most efficient using lasers with pulse-duration of ps or shorter. This is particularly true for precision hole drilling in aluminum.

In order to produce high quality holes in aluminum for the next generation of lightweight vehicles, we need to develop high-average power short-pulse lasers (with ps or shorter pulse-duration) and optimize the process parameters under vacuum or oxygen-free environments.

2) Analysis of the heat-affected-zone surrounding the fuel injector holes drilled by ultrashort-pulse laser

We produced 100-200 μm diameter holes in 9Cr-1MoVNb steel with pulse-durations of 0.5-to-25 ps and fluences of 2-15 J/cm^2. A few of the holes were analyzed by ORNL. We found that:

- Holes generated under low fluence (5 J/cm^2) and short pulse-duration (0.5 and 1 ps) conditions showed very little evidence of micro-structural change.
- More analysis of femtosecond-laser drilled holes is necessary to completely characterize the material changes.

It is evident that micron-scale holes with minimal heat-affected zone can be drilled using ultrashort pulse laser under short pulse (0.5-to-1 ps) and low fluence (5 J/cm^2) conditions. To achieve a drilling rate of interested to the US automakers, one must operate the laser at high repetition rate(>1000 pulse per second) with good beam quality. Minimum average power required for industrial-scale precision hole drilling on fuel injectors should be in the 5-to-50 W range.

3) Methods to drill small diameter (100's microns) holes in ceramics

Using a 405-nm laser with pulse energy of 1.1 mJ (3.5 J/cm^2) and pulse duration of 1 ps, we made several attempts to drill high quality 200-micron diameter holes in alumina, zirconia and other hard-to-work materials.

- At low fluence (3.5 J/cm^2), we were able to drill micron-scale holes in alumina to a depth of 0.3 mm but the drilling stalled out after 30 s with no evidence of breakthrough.
- At high fluence (70 J/cm^2), we were able to drill a 100 micron hole all the way through 9 mm of zirconia.

- We have also attempted to drill a 900-micron hole in zirconia using trepanning or "core-drilled" techniques. The drilling stalled out after approximately 4 mm depth due to losses of laser energy in reaching the bottom of the long, narrow slot, and due to the difficulty in the debris finding its way out of the hole.

- We were able to drill 3-mm depth holes in zirconia with no evidence of micro-cracking.

With the limited data on ceramic materials, we feel that the ultrashort-pulse laser operated under high fluence (~70 J/cm^2) and short pulse-duration (~1 ps) conditions can be used to precisely drill holes and machine fine structures on ceramic materials, such as alumina and zirconia. However, more test data are required to optimize the drilling and machining parameters for US auto-makers to manufacture parts for the next generation of vehicles.

5.2 Materials processed by LLNL's femtosecond laser system

The following table summarizes the types of metals, dielectrics, ceramics, and composites that we have machined using LLNL's femtosecond laser system as well as sample results and comments. Our experience includes both ceramics and composites, but that much more work is needed in these areas.

Metals, Dielectrics, Ceramics, and Composites Machined Using LLNL's Femtosecond Laser Systems

material	Type, size, processing	Comments
Fused silica, calcium fluoride, sapphire	Material removal threshold	Very thoroughly studied for laser fusion research
Teeth, hard tissue (bone)	300-μm holes through 1mm	Minimal collateral damage, minimal temperature rise, cuts great
Soft tissue	Skin, chicken meat, pig heart tissue	Cuts well with minimal collateral cell damage
High explosives	DOE secondary explosives up to 1 cm thick	Cut easily with no reactions
Plastics	Teflon, polymer, narrow cuts	Smooth cuts, no melting
Aerogel	Line cuts, cm deep	Some discoloration, but nice cuts
Fabrics	Shoe parts – suede, plastics, foam	Minimal melting, good edge quality
Ceramics and Metal Matrix	Silicon carbide, aluminum titanium carbide, aluminum/silicon carbide metal-matrix, 2-mm thick line cuts	*Cut fairly easily with high precision and good quality*, more work needed

Composites	Carbon-fiber epoxy, 2-mm Glass-fiber Ultem	*Cut fairly easily with high precision and good quality*, need careful optimization, more work needed
Stainless steel	304, 316, others, holes and lines, up to 1/8" thick, fuel injectors, stents	Rates slow compared with most other materials, good quality
Carbon steel	Rates and holes	Similar to stainless
Aluminum	Various types, up to 1/8" thick lines and holes	*Cut fairly easily with high precision and excellent quality*
Titanium, beryllium, aluminum foils	Small features (<5 μm) in foils to 125-μm thick	*Works great, pushing to 1-μm features*
Iron	Relay cores, 1x1x2 mm	Produced clean edges and minimal magnetic changes
Other metals	Copper, gold, platinum, palladium, titanium, tantalum, hastalloy, N5, nickel, neodymium, cerium, uranium	Cutting rates, holes and lines, demonstrations
Semiconductors	Silicon, gallium arsenide	Decent cuts and holes, more work needed

5.3 Future Directions

We propose a two-year plan to investigate issues important to automotive technology, including:

- fuel injectors drilling, focusing on backwall damage prevention, and evaluating spray pattern vs. taper (with Sandia Nat. Lab.)
- ceramics and composite cutting and drilling including aluminum-based metal matrix composites
- cutting of deep, thin slots for catalytic converter applications
- laser cleaning of metal surfaces and welding tests